U-TH DATING AND PHYSICAL PROPERTIES OF STALAGMITES FROM AMPHOE BAN RAI, CHANGWAT UTHAI THANI: PALEOCLIMATE IMPLICATION

Mr. Kampanart Jankham

A Report Submitted in Partial Fulfillment of the Requirements
for the Degree of Bachelor of Science
Department of Geology
Faculty of Science
Chulalongkorn University
Academic Year 2015

การหาอายุโดยวิธียูเรเนียม-ทอเรียม และคุณสมบัติทางกายภาพของหินงอก จาก อำเภอบ้านไร่ จังหวัดอุทัยธานี: ประโยชน์ด้านการเปลี่ยนแปลงภูมิอากาศในอดีต

นาย กัมปนาท จันทร์คำ

รายงานฉบับนี้เป็นส่วนหนึ่งของการศึกษาตามหลักสูตรปริญญาวิทยาศาสตรบัณฑิต
ภาควิชาธรณีวิทยา คณะวิทยาศาสตร์ จุฬาลงกรณ์มหาวิทยาลัย
ปีการศึกษา 2558

Date of Submission.....

Date of Approval.....

.....Senior Project Advisor

(Sakonvan Chawchai, Ph.D.)

Title: U-TH DATING AND PHYSICAL PROPERTIES OF STALAGMITES FROM AMPHOE BAN RAI, CHANGWAT UTHAI THANI: PALEOCLIMATE IMPLICATION

Researcher: Kampanart Jankham **Student ID:** 5532702023

Advisor: Dr. Sakonvan Chawchai

Department: Geology

Academic year: 2015

Stalagmite is the one of advantaged paleoclimate and paleoenvironmental implication proxies. Our purposes are study the physical properties of stalagmites from Amphoe Ban Rai, Changwat Uthai Thani and select the stalagmites for paleoclimate implication. We have surveyed 20 caves and observed its physical properties – shape, color, and texture. We collected 3 stalagmite samples, nearly symmetrical shape, in the same cave. Physical properties assessment was done both before and after cutting process which including of texture, color, growth layer. Following by drilling process, we drilled 8 points and each points were replicated. Powdered samples went to the chemistry and measurement process via U-Th method. The ages shows the precipitation in part of late Pleistocene epoch (87000-105000 a. BP) and the large error (±970-7700 a.). Consequently, the time interval between top and bottom of each samples were overlapped. The precipitation of calcite might occur in open system in which disequilibrium that lead $^{230}Th/^{232}Th$ ratio ranges 27-273 and ^{238}U concentration ranges 40-181 ppb. Generally, the low of $^{230}Th/^{232}Th$ ratio represent a contamination (Jeffrey et al., 2004) and ^{238}U concentration should be at least 100-200 ppb. (Shen et al., 2002; H. Cheng et al., 2013). These induce the large error and unsuitable for study further. Eventually, this study reveals that this area consists of the oldest stalagmite in Thailand by now and all of the samples provide the age nearly with each other which represent the precipitation ages of all samples and might be composed of variety ages but undiscovered.

Keywords: Stalagmite, U-Th method, Paleoclimate

หัวข้องานวิจัย : การหาอายุโดยวิธียูเรเนียม-ทอเรียม และคุณสมบัติทางกายภาพของหินงอก จาก อำเภอบ้านไร่ จังหวัดอุทัยธานี: ประโยชน์ด้านการเปลี่ยนแปลงภูมิอากาศในอดีต

ผู้ทำการวิจัย : นายกัมปนาท จันทร์คำ **รหัสประจำตัวนิสิต** : 5532702023

อาจารย์ที่ปรึกษา : ดร. สกลวรรณ ชาวไชย

ภาควิชา : ธรณีวิทยา

ปีการศึกษา : 2558

หินงอกเป็นหลักฐานทางธรณีวิทยาที่สำคัญอย่างหนึ่งในการนำมาศึกษาการเปลี่ยนแปลงสภาพสิ่งแวดล้อมและสภาพภูมิอากาศบรรพกาล งานวิจัยนี้มีวัตถุประสงค์เพื่อศึกษาคุณสมบัติทางกายภาพ การหาอายุและประเมินศักยภาพของหินงอกเบื้องต้น ในอำเภอบ้านไร่ จังหวัดอุทัยธานี เพื่อประโยชน์ต่อการคัดเลือกหินงอกในการศึกษาด้านการเปลี่ยนแปลงภูมิอากาศบรรพกาล โดยทำการสำรวจถ้ำจำนวน 20 ถ้ำ และสังเกตลักษณะทางกายภาพของหินงอก คือ รูปร่าง สีและเนื้อหิน หลังจากการสำรวจได้เลือกเก็บตัวอย่างหินงอกที่มีรูปร่างเป็นแท่งตรงและสมมาตร 3 ตัวอย่างจากถ้ำเดียวกัน โดยบันทึกข้อมูลลักษณะกายภาพของหินทั้งก่อนและหลังการตัดตัวอย่างเพื่อดูโครงสร้างภายในของหินงอก (เนื้อหิน สี และเส้นการเจริญเติบโต) จากนั้นทำการเจาะผงหินงอกทั้ง 3 ตัวอย่าง โดยแบ่งเป็น 8 ตำแหน่ง และนำไปหาอายุโดยวิธียูเรเนียม ทอเรียม โดยทำซ้ำตำแหน่งละ 2 ครั้ง ผลการหาอายุพบว่าหินงอกทั้งสามตัวอย่างมีอายุการสะสมตัวในช่วงตอนปลายของสมัยไพลสโตซีน (ประมาณ 87000-105000 ปีก่อนปัจจุบัน) แต่มีค่าความคลาดเคลื่อนของอายุค่อนข้างสูง (ประมาณ ±970-7700 ปี) ทำให้ค่าอายุในช่วงด้านบนและด้านล่างของหินงอกในตัวอย่างเดียวกันมีการซ้อนทับกัน อาจเนื่องมาจากแร่แคลไซต์ของหินงอกมีการสะสมตัวในสภาพแวดล้อมแบบเปิดที่ไม่อยู่ในสภาวะสมดุล ซึ่งเป็นสาเหตุให้สัดส่วนของ $^{230}Th/^{232}Th$ มีค่าอยู่ระหว่าง 27-273 และปริมาณของ ^{238}U อยู่ระหว่าง 40-181 ppb. โดยสัดส่วนของ $^{230}Th/^{232}Th$ ที่น้อยแสดงถึงการปนเปื้อนนอกระบบ (Jeffrey et al., 2004) และปริมาณ ^{238}U ควรมีอย่างน้อย 100-200 ppb (Shen et al., 2002; H. Cheng et al., 2013). ทำให้อายุที่ได้ออกมามีความคลาดเคลื่อนสูงและไม่เหมาะสมที่จะศึกษาสภาพภูมิอากาศบรรพกาลในเชิงลึกต่อไป แต่อย่างไรก็ตามงานวิจัยนี้แสดงให้เห็นว่าพื้นที่นี้มีหินงอกที่มีอายุเก่าแก่ที่สุดที่ได้มีศึกษาในประเทศไทยและการที่อายุของทั้ง 3 ตัวอย่างให้อายุที่ใกล้เคียงกันนี้แสดงถึงช่วงเวลาการสะสมตัวของหินงอกในถ้ำนี้ ซึ่งอาจมีช่วงอายุอื่นด้วยแต่ยังไม่ได้ค้นพบ

คำสำคัญ: หินงอก, วิธียูเรเนียม-ทอเรียม, สภาพภูมิอากาศบรรพกาล

ACKNOWLEDGEMENTS

Firstly, I really appreciate to people in Amphoe Ban Rai, Changwat Uthai Thani who always understand and guide our team to find the caves and contribute to the successful complete of field survey. I also thank Asst. Prof. Dr. Pitsanupong Kanjanapayont, Asst. Prof. Dr. Vichai Chutakositkanon, and Mr. Peerapong Sritangsirikul for guidance and helping in collecting sample for the first time. Especially Mr.Siripong Thonongto (Aj. Mod) of Panda camp and his family. Your kindness and a warm welcome are never be forgotten.

I would like to express my deep grateful to Earth Observatory of Singapore's team. I am supported by Earth Observatory of Singapore's team. Asst. Prof. Xianfeng Wang and his team that including of Hong-Wei Chiang, Liu Guangxin, Yuan Shufang, and Ke Lin. Guidance, worth critiques, and supporting of dating and accommodating cost are very helpful to my project. These obligation is respectable.

I acknowledge much helpful and encouraging as always to my all of colleagues (GEO'56) and juniors (GEO'57). Particularly my partner, Miss Warisa Paisonjumlongsri, who has collaborated from the beginning until the end.

To my advisor, Dr. Sakonvan Chawchai, I would like to express my deep gratitude for her dedication, patient, and guidance. She treat us like a brother like a sister and she is the best teacher ever. I also thank Raphael Bissen who helping me at writing report and guidance.

Finally, my incessant encouragement belongs to my family that supported me to break through of the study.

TABLE OF CONTENTS

Page

ENGLISH TITLE

THAI TITLE

ABSTRACT (English)

ABSTRACT (Thai)

ACKNOWLEDGEMENTS

TABLE OF CONTENTS

LIST OF TABLE

LIST OF FIGURE

CHAPTER

I	INTRODUCTION	1
	1.1 Rationale	1
	1.2 Objectives	3
	1.3 Study area	3
	1.4 General Geology	4
	1.5 Literature reviews	6
II	Methodology	17
	2.1 Fields study	18
	2.2 Preparing samples	20
	2.3 Laboratory at Earth Observatory of Singapore	23
III	Results	39
	3.1 Physical properties assessment	39
	3.2 Chronology	44
IV	Discussions	46
	4.1 Physical properties assessment	46
	4.2 Uncertainly errors and uranium-thorium content	50
V	Conclusion	54

REFERENCES 56

LIST OF TABLE

TABLE		Page
1	Grid location of caves.	19
2	Summary of physical properties of 3 samples	43
3	^{230}Th dating results of BR 1-3 Stalagmites from BR cave, Western Thailand. Measured by MC-ICP-MS and the error is 2s error.	45
4	Quantity of average element of point 10-11-12 of Warisa's study (Fig.39).	40
5	Percent errors of ^{230}Th Age	51
6	Comparison of ^{230}Th / ^{232}Th ratio and ^{238}U content of our study with others.	52

LIST OF FIGURE

FIGURE		Page
1	Location of study area and monsoon influenced.	4
2	Relationships of speleothems to external climate-drivers (adaptedfrom Houghton et al., 2001) (b) Dissolutional and precipitative zone (adapted from Tooth, 2000). (c) Processes in the cave environment. (d) Longitudinal section of inner stalagmite.	6
3	Flowstone, Stalactite, and stalagmite.	7
4	^{230}Th / ^{238}U activity ratio versus age. A high initial 234U/238U ratio (expressed in delta units) accounts for an extended dating range as secular equilibrium is reached after a longer time period (after Richards and Dorale, 2003). Most speleothems show δ^{234}U values between ca. 100 and 1200.	8
5	The 4n+2 chain of ^{238}U	9
6	Comparison of various dating method which including of ^{14}C, ^{238}U-^{234}U-^{230}Th, α-counting and ^{238}U-^{234}U-^{230Th} (This study). As you see in the table, this study has less error than every method and the age can reach more than ^{14}C dating method.	11
7	Central depression is visible on the stalagmite apex, surrounded by small holes, gours and other irregular shaped cavities (in situ stalagmite at Te'omim Cave)	12
8	Axial and off-axis macroholes; note the growing layers bending towards the axial holes, and the clear cutting of the growing layers by the off-axis holes, in polished surfaces (middle) or in petrographic thin sections (right).	14

LIST OF FIGURE (*Continued*)

FIGURE		Page
9	Calcite coatings and new crystals growing epitaxially within off-axis holes. A) SEM imaging; B) new crystals grow to form new coatings along the hole's walls; C and D) no coatings are visible, new crystals grow directly on the holes' substrate. Note the stalagmite growth layers cut by the holes.	14
10	Secondary Electron Scanning Micrographs of: A) bacteria coating an axial hole surface, forming biofilms along the wall of the axial hole (B); C) organics, fillaments and coccoid cells on an off-axis hole surface (note weathered calcite crystals); D) clean surfaces of calcite within and around micro-inclusions.	15
11	Comparisons of (a) Dipole mode index (DMI) (filled grey line) (Abram et al., 2008), and (b) ENSO (filled grey line; Y axis is reversed) (Li et al., 2011) with NJ-0901 growth rate series (black lines). All data were normalized by their respective standard deviations. Pearson's correlations (r-values) and statistically significant values (bold print) are shown. (c) Thirty-one-year sliding correlation of growth rate with DMI (black line) (Abram et al., 2008) and ENSO (grey line) (Li et al., 2011). 95% confidence levels are indicated using grey bars. The vertical dashed line indicates the boundary at 1905 AD.	16
12	Cave's location (red circle: survey caves; yellow: study site in this study.	18
13	Standing sample (BR3).	20
14	Samples before cutting.	21
15	BR1 sample.	21
16	BR2 sample.	22

LIST OF FIGURE (*Continued*)

FIGURE		Page
17	BR3 sample.	22
18	Washing sample in Ultrasonic cleaner machine with Deionized water.	23
19	Drilling must only do in Air clean hood.	25
20	Drilling heads.	25
21	Acid and Methanol for wash drilling head.	26
22	Drilling sample.	26
23	Scientifc balance.	27
24	Vials for powder samples.	27
25	Atmosphere in sampling room.	28
26	Position of drilling.	28
27	Chemistry room.	37
28	Chemistry room.	37
29	Vial test.	38
30	(a.) Surface skin of BR1 sample and linear of longitudinal section for cutting. (b.) scanned cut-samples show inner skin, texture, and color of growth layers.	39
31	Drilling positon of BR 1.	40
32	Drilling positon of BR 2 sample.	40
33	(a.) Surface skin of BR2 sample and linear of longitudinal section (b.) Scanned cut-samples show inner skin, texture, and color of growth layers.	41
34	(a.) Surface skin of BR3 sample and linear of longitudinal section which was cut. Photo was taken by camera. (b.) cut-samples show inner skin, texture, and color of growth layers. Photo was scanned by printer.	42

LIST OF FIGURE (*Continued*)

FIGURE		Page
35	Drilling positon of BR 3.	42
36	Sketch illustrating the gradual opening of secondary voids in the primary columnar calcite.	46
37	Cavities in BR 1 (lower part; right).	47
38	(a.) Cavities in BR 2 (lower part; left) (b.) Cavities in BR 2 (lower part; right).	47
39	Illustrates the oxidation layer on BR 2; the upper right part (3.1 cm from top)	49
40	The discontinuity layer as red, yellow, green, and blue lines on BR 2; upper right part.	49
41	The altered sample of BR 3 (lower part; left) and BR 2 (lower part; left) after cutting.	53

Chapter 1

Introduction

1.1 Rationale

In the present day, there is extreme variation in temperature and rainfall precipitation around the world. Drought and flooding events have occurred in different regions. So global warming and climate change make people aware of its important. For Thailand, the Thai meteorological department has recorded the amount of precipitation and temperature about 50 years ago, therefore the information for long-term climatic change has limited. According to the limited statistic data, the prediction of climatic events forecasting becomes difficult.

The environment and topography from each region in Thailand are quite different. There are few paleoclimatic studies within Thailand during the last two decades. Most of information came from lakes study, which reconstructed paleoenvironmental and paleoclimatic change during the Holocene epoch (c. 10,000 years BP). However, the paleoclimatic data within Thailand are still scarce. This makes it difficult to compare to other monsoon regions (Penny, 1998; White et al., 2004; Buckley et al., 2007; Boyd, 2008; Marwick and Gagan, 2011; Wohlfarth et al., 2012; Chawchai et al., 2013; 2015; Chabangborn et al., 2014).

Caves can be found around Thailand especially in the southern and western part of Thailand, including tourism caves and closed caves. The formation of cave occurred by rain that composed of weak acid inside, dissolve carbonate rocks e.g. limestone, dolomite and/or gypsum. This made variety of cavities and holes developed to cave. Besides, the beauty of caves, they also keep a treasure of science in Speleothems as we see many types in the cave such as Stalagmites, Stalactites, and Soda straw, etc.

During the last decade, scientist found the literally of stalagmites which used to study paleoclimate. Characteristic of its deposit as growth layer like a tree rings keeps many secrets of nature, for example; seasonal variety, monthly mean $\delta^{18}O$ data of atmospheric moisture, ecosystem and soil zone overlying the cave, modeling of aquifer, and precipitation of calcite or aragonite crystal (Fairchild et al., 2006). However, a suitable stalagmite for paleoenvironmental and paleoclimate research has to deposit in a closed system, for example, in the cave with less human activity. The suitable caves therefore have narrow entrance, less of air circulation, high humidity, and deep and long chambers. This still needs more observation and exploration for those caves.

Stalagmites deposited in karst environment can continually grow up to several thousand years (Fleitmann et al., 2008). With the latest technology can help us to study physical and chemical properties of stalagmites such as stable isotope, trace elements, and annual ring. In addition, stalagmites also compose of Uranium and Thorium as trace elements that can be utilized to measure the age by U-Th dating method (Culver, D., & White, W., 2005). However, the cost of U-Th dating method is quite expensive and both elements can be disturbed easily by the nature. To assess the basic physical properties such as color, texture, and shape are the fundamental criteria of sample selection for the research used.

Previously, only one stalagmite record in Thailand at Namjang cave, Pang Ma Pha district, Mae Hong Son province, covered the last 1700 years ago, has been reconstructed (Cai et al., 2010 and Muangsong et al., 2014). The amounts of oxygen isotope and grey level of growth layer were studied. The stalagmite and hydrometeorological records at the local meteorology of Mae Hong Son station and nearly station were correlated. The results shown that northwestern Thailand has very complicated environment and climate (Muangsong et al., 2014). Most of precipitation periods are between August and October.

Possibly, this region is influenced by various monsoon directions, El Niño Southern Oscillation, and heterogeneous intraseasonal patterns.

Eventually in the present still needs more paleoenvironmental and paleoclimatic data from other regions in Thailand for better understanding of long-term climate dynamic in this region. This project aims to develop fundamental knowledge for a better understanding of natural stalagmite in Thailand for paleoclimatic study, which is still heavily under-sampled.

1.2 Objectives

The main objective of this study is to decipher how suitable stalagmite samples for paleoenvironmental and paleoclimatic study are. To address these questions, the primary aims for this study are as follows:

1.2.1 Survey caves in Ban Rai district, Uthai Thani province.

1.2.2 Study the basic physical properties (color, texture, and shape) of stalagmites

1.2.3 Measure the selected stalagmites with U-Th dates (3 samples).

1.3 Study area

The study area is located on western part of Thailand at Ban Rai district, Uthai Thani province where several limestone mountains can be found. From preliminary survey during field study (FIELDWORK II., 2015), there is lot of caves that could be suitable for paleoclimatic research. This area is influenced by the northeast-southwest monsoon and also tropical cyclone.

A general climate in this region ranges from subtropical to tropical climate. General climate is divided into 3 seasons: summer season (February-May), rainy season (May-October) and winter season (October-February). During raining season, in the western part has more rainfall than eastern part because of its influence of southwest monsoon. Mean annual rainfall is 1770.3 millimeters with average 105 raining days and maximum and minimum temperatures are 36°C and 17.6°C, respectively.

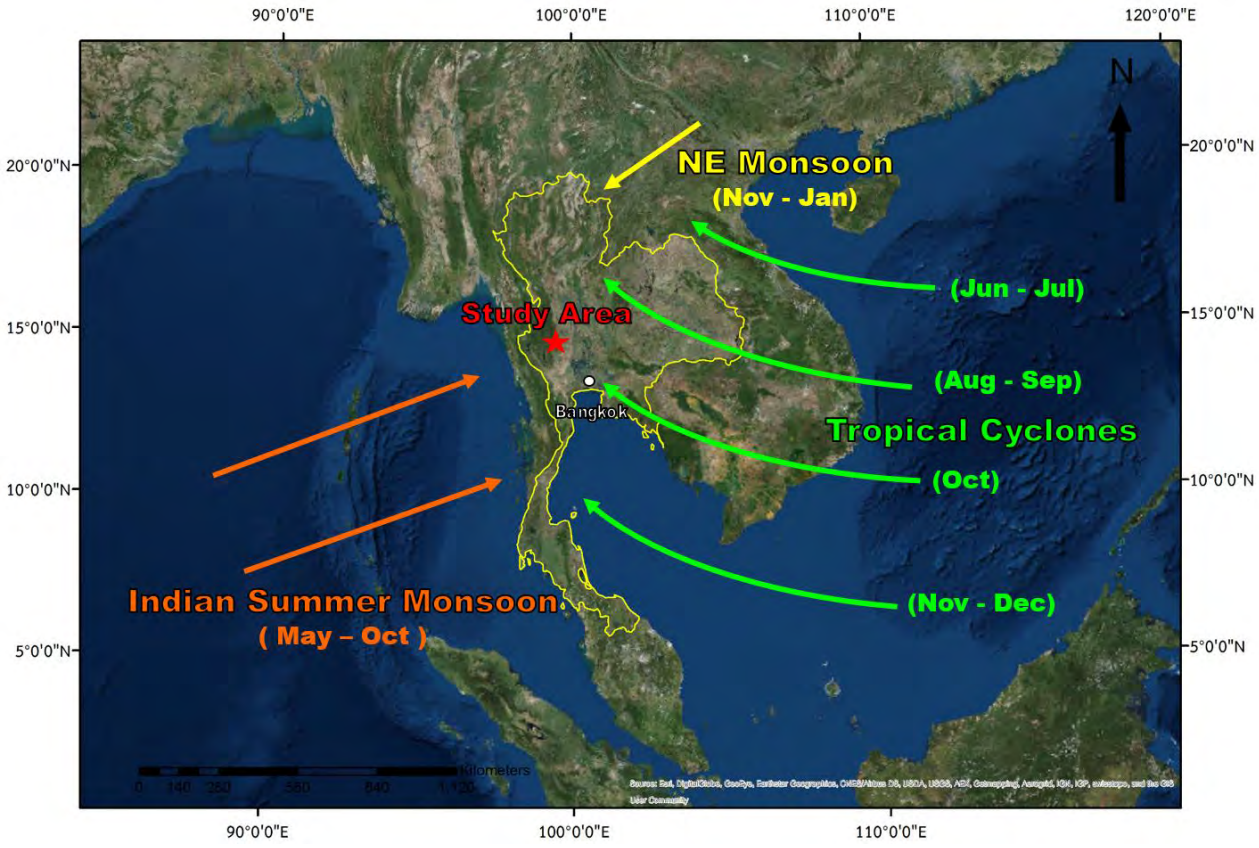

Figure 1. Location of study area and monsoon influenced.

1.4 General Geology (DMR, 2008)

Uthai Thani province is located at the northwest part of central region. In geology terms, the western part of Uthai Thani lies continually from Tak province–Inthanon-Tak range that placed on Shan-Thai microplate. This microplate composed of sedimentary rocks, metamorphic rocks, igneous rocks, and unconsolidated sediments. The geochronological age covers Precambrian period (more than 570 Ma), Cambrian period (505-570 Ma), Ordovician period (439-505 Ma), Silurian-Devonian (360-438 Ma), Carboniferous period (286-360 Ma), Permian period (245-286 Ma), Triassic period (210-245 Ma), and Quaternary period (0.01-1.6 Ma). The quoted periods has deposited in continents and oceans. Deformation of rocks was made by intrusive of igneous rocks. The uplift process was caused of weathering, erosion, and deposition of unconsolidated sediments on the eastern part.

Lithology and texture of limestone in the study area rock in the cave:

Argillaceous limestone shows black in fresh color. Weathered surface shows argillaceous band obviously. Fossils Nautiloid and Crinoid indicated Ordovician period. Some area shows slight deformation as calcite recrystallized and another area shows metamorphism process as calc-silicate rock and marble. The argillaceous limestone in some area shows dolomitic texture or contains big calcite crystal. Calc-silicate rock shows black-brown in fresh color, big calcite crystal, and banding separated minerals composition. When compared lithology, rock types, structural geology, and stratigraphic correlation, this rock unit indicates Tha Manao formation in Ordovician period. Tha Manao formation has a type section in the north of Kanchanaburi province. This formation is spread around southern and western part of Ban Rai district and Huai Kha Khaeng Wildlife Sanctuary. Bedding lies in northwest-southeast direction. Geology of this area composed of mudstones and argillaceous limestone in lower part and overlaid by quartzite and quartz-schist of Chao Nen formation. Then, it gradually changed into limestone cliff and carried of round-chert inside. Next, there is a grey thin limestone that shows recrystallization and some part deformed into marble. After that, there is overlaid by calc-silicate that interfingered with thin sandstone layer and then gradually changed into massive limestone, which interfingered with quartzite and phyllite. The most uppermost part of this formation include of light grey to grey thin limestone which is laid continually under white shale (Silurian-Devonian). Fossil evidences show that the age of Tha Manao formation is in Ordovician period (505-438). Early Ordovician fossils are Cystoids and absence of Conodonts that is index fossil of middle Ordovician. Late Ordovician fossils are *Armenoceras myanmarense* sp.

1.5 Literature reviews

Formation of stalagmite:

Fairchild et al., 2006 had classified a process that influenced of deposition of stalagmites into 5 factors: atmospheric, vegetation/soil, karstic aquifer, primary speleothem crystal growth and secondary alteration. These processes make characteristic of stalagmites different in another area. The majority of study focuses on $\delta^{18}O$ signals which are the important analytical factor for atmospheric humidity and also including of isotope elements such as carbon and trace elements. So stalagmites kept these signals in

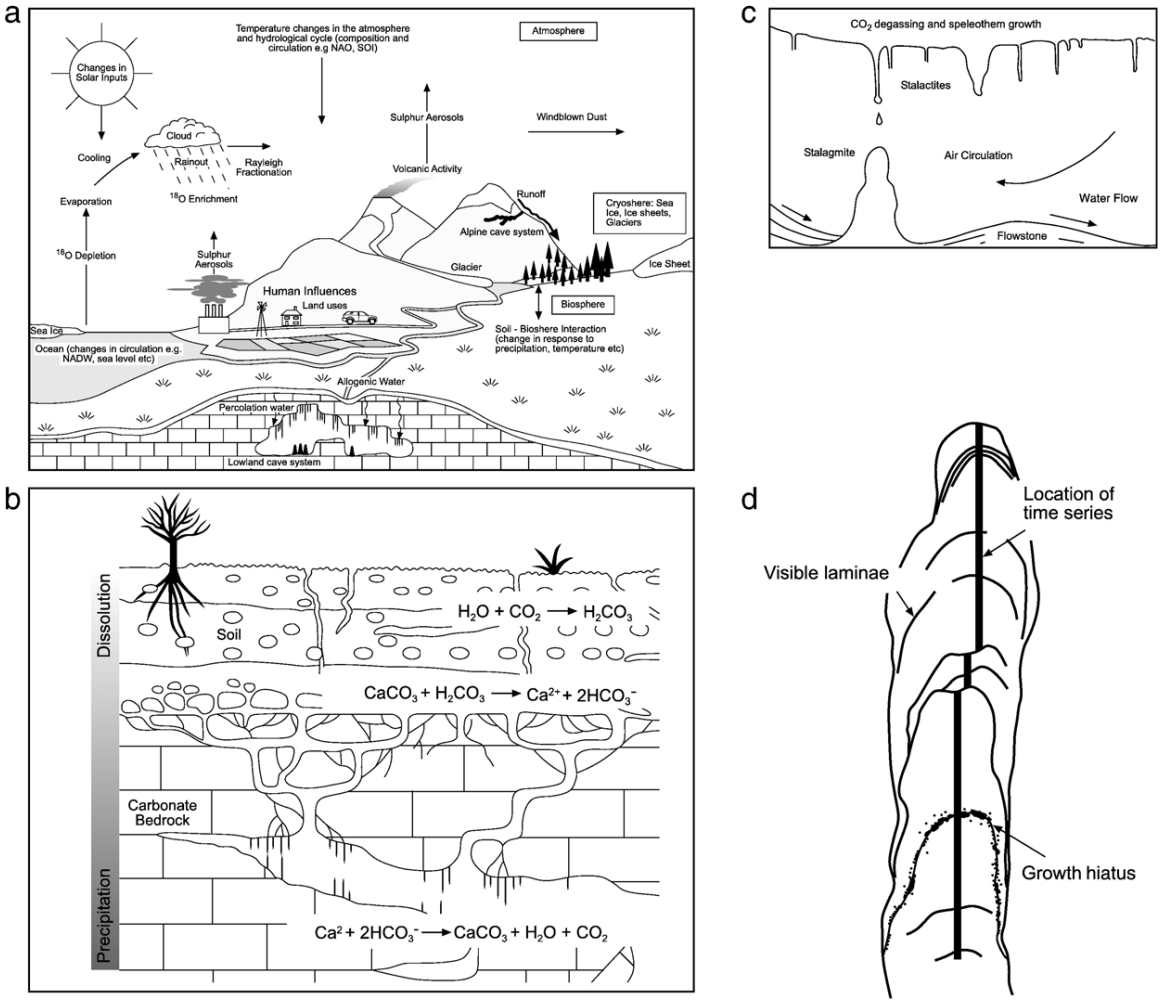

Figure 2. (a) Relationships of speleothems to external climate-drivers (adapted from Houghton et al., 2001) (b) Dissolutional and precipitative zone (adapted from Tooth, 2000). (c) Processes in the cave environment. (d) Longitudinal section of inner stalagmite.

its growth layers. The environment above the cave has influenced the karst (Fig. 2a). Especially epikarst or subcutaneous zone that have fissures to feeding drips water. In generally, Figure 2b shows two regions that have different geochemical function. Dissolution zone is influenced by high pressure of CO_2 that relative with vegetation and soil above the karst. Precipitation zone is zone of supersaturated CO_2 and then the speleothems are precipitated by degassing process of CO_2 (Fig. 2c). Even the temperatures is a minority influence but changing of quantity and chemistry of dripping water or varying CO_2 concentration of the cave atmosphere are notable.

There are 3 principles of speleothems that uses for paleoenviromental studies. The first is flowstone which deposits on floor or walls of cave. Sheets of flowing water derives from fissures and extend laterally. Consequently, Non-uniform of calcite growth rates is not suitable for study. The second is hollow cylindrical *soda-straw* stalactices. It's often associated with seepage zones on cave ceilings, but very delicate and young age. The third is stalagmites which most researcher prefer. Growing upward time series, U-series methods typically provide the basis of the age model. Even long-term growth rates can be nearly linear, there are many factors that preceding the deposition such as varying growth rate that evoking different feature composed.

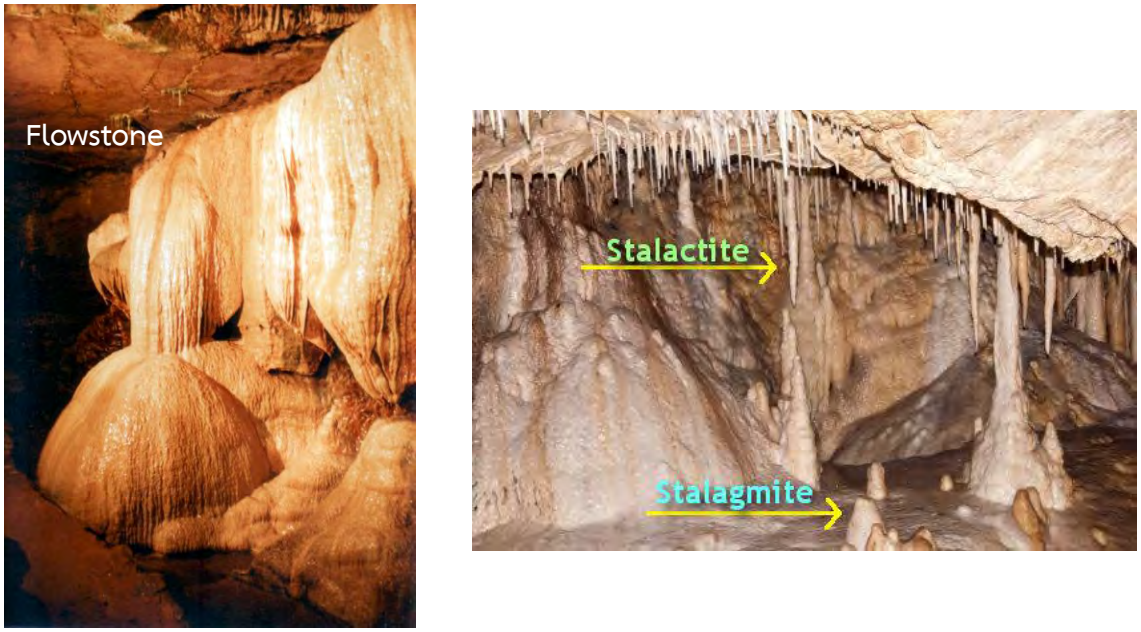

Figure 3. Flowstone, Stalactite, and stalagmite.
(http://financialspots.com/2016/02/07/what-is-a-stalagmite/)

U-Th dating methods:

Regarding to The Encyclopedia of caves (Culver, D., & White., 2005), around 1950s radiocarbon (^{14}C) was applied as a method with dripstone but the results showed rough estimate of their formation age and sample older than 50000 years cannot be dated using this method. Then four decades later, U-series or Uranium-Thorium method is improved and become the most highly respected of chronological techniques and valuable for paleoenvironmental and paleoclimatical study.

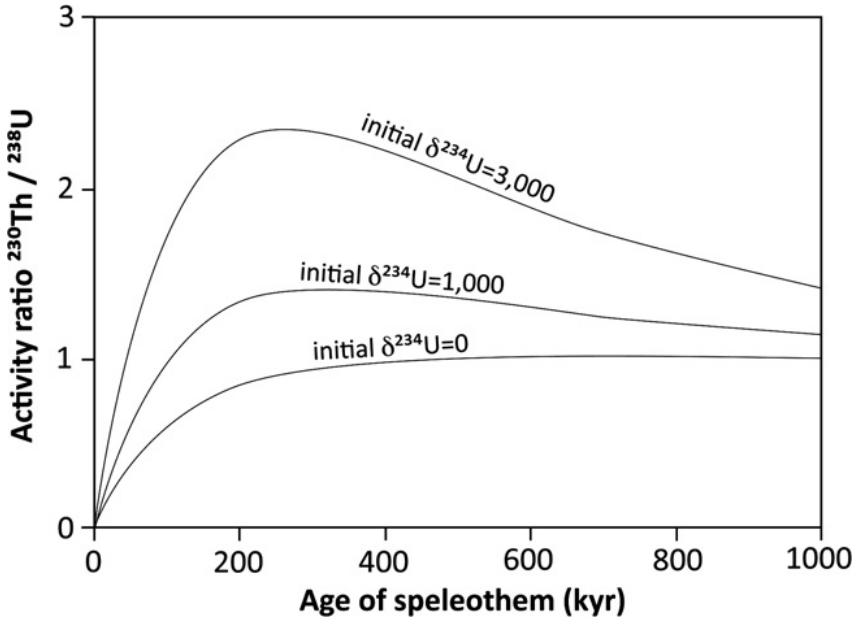

Figure 4. ^{230}Th / ^{238}U activity ratio versus age. A high initial 234U/238U ratio (expressed in delta units) accounts for an extended dating range as secular equilibrium is reached after a longer time period (after Richards and Dorale, 2003). Most speleothems show $\delta^{234}U$ values between ca. 100 and 1200.

According to naturally occurring of U isotopes, there are 3 isotopes: ^{238}U, ^{235}U, and ^{234}U. The isotopic abundant depend on the decay laws in which starting with the parent isotope ^{238}U and decay follows the Figure 5. In the measurement process, we focus only: ^{238}U, ^{234}U, and ^{230}Th.

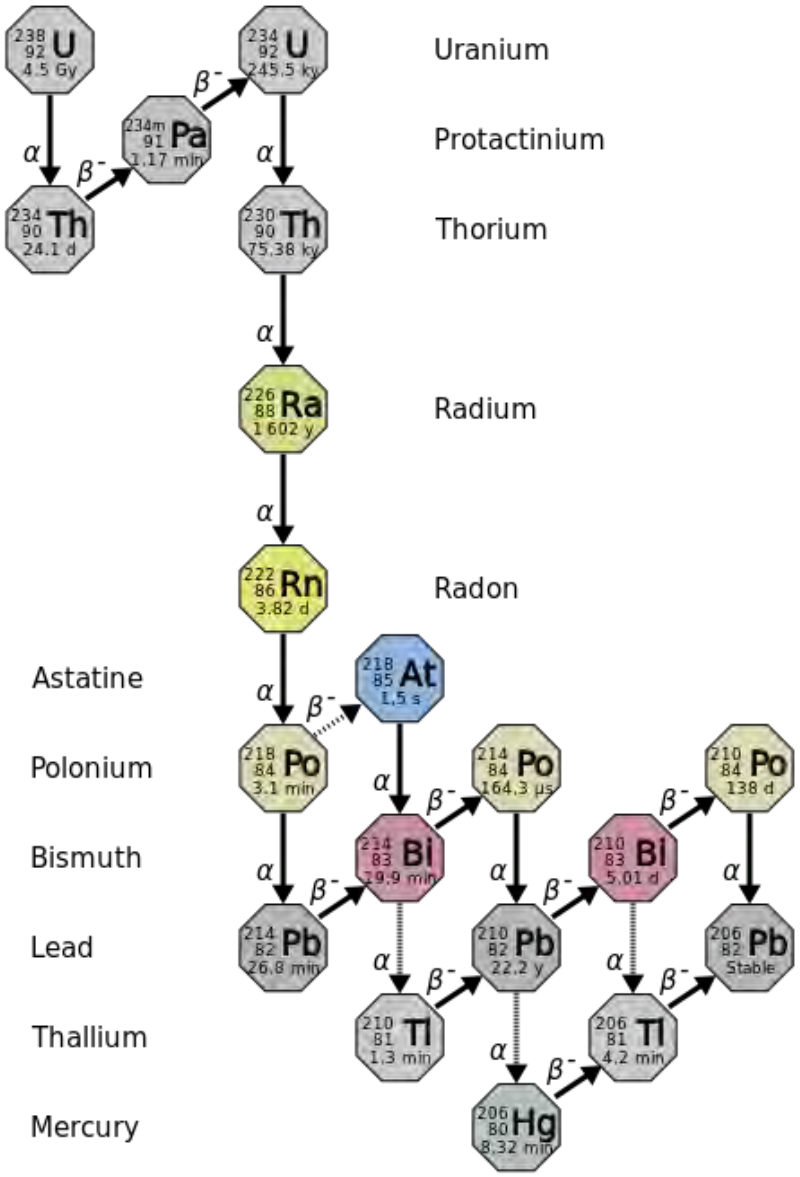

Figure 5. The 4n+2 chain of ^{238}U

(https://en.wikipedia.org/wiki/Decay_chain#/media/File:Decay_Chain_Thorium.svg)

The initial ratios of ^{230}Th / ^{238}U as Figure 4 depend on geochemical characteristic of sample. The older sample you had, the higher ratio does. This method can reach to 600,000 – 700,000 years. After starting decay, an initial state of disequilibrium between U and Th isotope has occurred. In addition, thorium is insoluble in water and tends to be absorbed on particles but U is soluble and transported within solution. Therefore, in the initial decay state we found a few of thorium or approach to zero but in an older sample,

thorium tends to get higher. In ideal conditions, when U atoms are incorporated in lattice of the carbonate crystal, ^{230}Th only originates from ^{238}U as Figure 5 and "the U-Th clock" was started. These condition must be kept in closed system because there must be increase or decrease these isotopes. As a consequence, the suitable sample should not be recrystallized or dissoluted. According to ^{232}Th, it is the most common isotope of thorium in the nature and can preserve implicitly in stalagmites. This isotope has the longest half-life (1.4×10^{10} years) which more than age of earth—primordial nuclides. In measurement, ^{232}Th must be correct by the ^{232}Th concentration and initial ^{230}Th / ^{232}Th activity ratio for measurement the literally ratio of ^{230}Th / ^{238}U. In the present, there are 2 machine that are used for U-Th measurement; Thermal ionization mass spectrometry (TIMS) and single/multi collector inductively coupled plasma-mass spectrometer (ICP-MS). The ICP-MS has an advantage more than TIMS. For example, reduced sample size, shorter analysis time, and increased sensitivity due to higher ionization efficiency. The precision of this measurement usually reported at the 2-sigma uncertainly level that means 95% of sample fall into the age ± error. For instance, the error should be ±10 a at 10 ka, ±100 a at 130 ka, ±300 a at 200 ka, ±1 ka at 300 ka, ±2 ka at 400 ka, ± 6 ka at 500 ka, and ±12 ka at 600ka. (H. Cheng et al., 2013).

According to the suitable proportion of each element for dating by MC-ICP-MS, Uranium contents should be rich at least a few hundred ppb (Shen et al., 2002; H. Cheng et al., 2013). So in the calculation proportion in sample, the machine will collect the ^{235}U instead of ^{238}U because ^{238}U need more high beam energy that make the cost get more expensive and the ^{238}U/^{235}U ratio is a constant number 137.88, (Edwards et al., 1987). According to a spikes and standards, Spike is an obtained-isotope solution that we know the exactly proportion and can compare with another isotope in age calculated process. In the spike, it compose of artificial matter which mixed of uranium and thorium isotope. ^{229}Th spike is used as a standard. The machine will calculate as a ratio of ^{230}Th / ^{229}Th and

^{232}Th / ^{229}Th which leading to the calculation of ^{230}Th age. In uranium isotope standards, we determine the ^{236}U-^{233}U as spike which including of ^{233}U/^{235}U, ^{234}U/^{235}U, and ^{236}U/^{235}U standard (H. Cheng et al., 2013). By the way, the proportion of spike and standard is depend on each laboratory. If uranium content is low, weight of spike should be 1/2-1/3 mass sample—close to the U-Th numbers in sample.

According to Edwards et al., 1987, this paper illustrated how to measure the age by U-Th dating method in corals. The purposes are to reduce the sample and increase the certainty of the age. Moreover, they also explain some chemistry procedures such as the relationship of Uranium stable isotopes which used to be a Spike and be a standard solution, preparation of digestion process, needless elemental separating process, U-Th collecting for measurement process, and the advantage of ^{238}U-^{234}U-^{230}Th dating (Fig.6). After chemistry is measurement process that run by Mass Spectrometer. The results show amount of ^{38}U and ^{23}Th ranges in 9-14 nmol/g and 0.083-1.57 pmol/g, respectively. So that made the less uncertainty age and can be reach to 500,000 years.

Coral ages using different methods or techniques [a]

Sample	^{14}C [b] (conventional)	^{14}C [c] (corrected)	Ring counting	^{238}U-^{234}U-^{230}Th (α-counting)	^{238}U-^{234}U-^{230}Th (this study)
TAN-E-lg	270 ± 120 y (1)	30–70, 180–270, or 300–500 y	176–182 y (1)	–	180 ± 5 y
CWS-F-1	980 ± 120 y (1)	780–1010 y	–	–	845 ± 8 y
CH-8	8990 ± 120 y (2)	~10,000 y	–	–	8294 ± 44 y
AFS-12 A	–	–	–	129 ± 9 ky (3)	122.1 ± 1.1 ky
B				129 ± 9 ky (3)	122.7 ± 1.3 ky
C				129 ± 9 ky (3)	124.5 ± 1.3 ky
E-T-2	–	–	–	141 ± 16 ky (4)	129.9 ± 1.1 ky
E-L-3	–	–	–	141 ± 16 ky (4)	125.5 ± 1.3 ky

[a] All errors are 2σ. Ages refer to the ages in 1986 (C.E.). Numbers in parentheses refer to the following sources: (1) F.W. Taylor (written communication), (2) Taylor et al. [39], (3) Ku (unpublished), (4) Bloom et al. [40].

[b] ^{14}C ages are as reported by the sources in radiocarbon years using the 8033 year mean life; no corrections have been made for natural fractionation of carbon isotopes, the difference between ^{14}C/C in surface water and the atmosphere, or differences in initial ^{14}C/C.

[c] ^{14}C ages have been corrected by us to dendroyears using the curves of Stuiver [68] for TAN-E-lg and CWS-F-1 and assuming a ^{14}C/C initial ratio from Klein et al. [69] for tree rings ~ 8000 years old. No corrections have been made for natural fractionation of carbon isotopes or the difference between ^{14}C/C in the surface water and the atmosphere.

Figure 6. Comparison of various dating method which including of ^{14}C, ^{238}U-^{234}U-^{230}Th, ∝-counting and ^{238}U-^{234}U-^{230Th} (This study). As you see in the table, this study has less error than every method and the age can reach more than ^{14}C dating method.

Dissolutions process:

From Shtober-Zisu et al., 2014, most of stalagmites are usually composed of fluid inclusion inside. Primary porosity was found within crystals and along crystal boundaries, elongated parallel to the c-axes and the growth axis of the stalagmite (Zhang, 2007) and also found concentrated within growth, and along hiatuses or weathered surface. The diameter ranges from ~20 nm to >1 mm in diameter (Kendall and Broughton, 1978), and can constitute up to ~0.1 wt% of the speleothem (Schwarcz et al., 1976). There are 2 types of macroholes that trapped water; Axial holes which growing simultaneously along

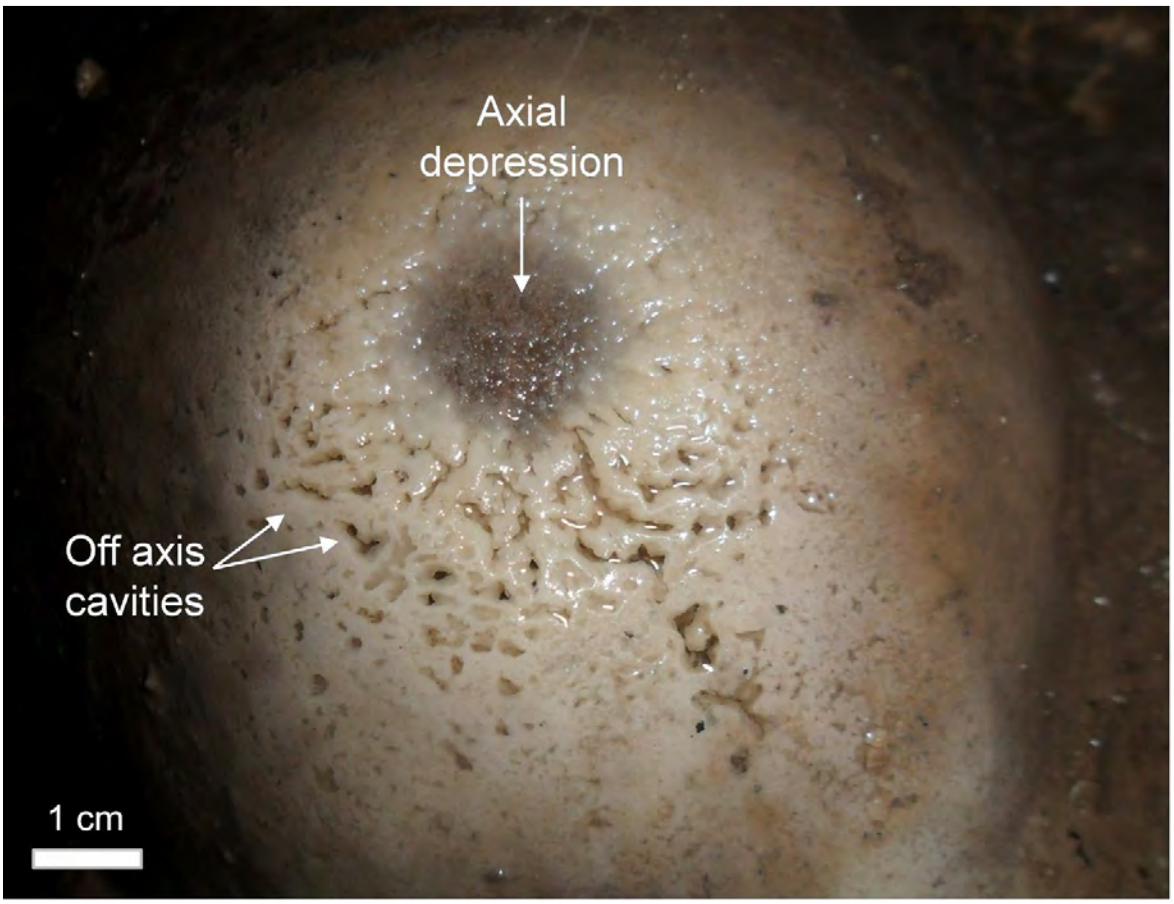

Figure 7. Central depression is visible on the stalagmite apex, surrounded by small holes, gours and other irregular shaped cavities (in situ stalagmite at Te'omim Cave)

growth layers in a slow rate precipitation. Off-axis holes (OAHs) which growing simultaneously along growth layers but temporary and non-connected.

In this study, they studied 26 stalagmites from different climate regions and used X-ray computed tomography (CT) for looking the internal structure of solid objects—3-D geometry was obtained. The results showed characteristics of macroholes—Axis holes and Off-axis holes (OAHs), Corrosional and depositional features in macroholes, Microbial colonization, and classification of macroholes. So holes is a cavity that has diameter more than 1 mm. The characteristics of Axis holes are elongated parallel to the growth axis and uppermost of hole may connect with the central depression (Fig. 7), its diameter range from 0.5-0.4 cm and length is more than 1 cm. The marked feature is downward bending of growth layers towards to the holes. According to Off-axis macroholes (OAHs), it is developed away from the stalagmite axis, cut through the growth layers, hardly extend to the surface, and usually more rounded and smaller than Axis holes (Fig.8).

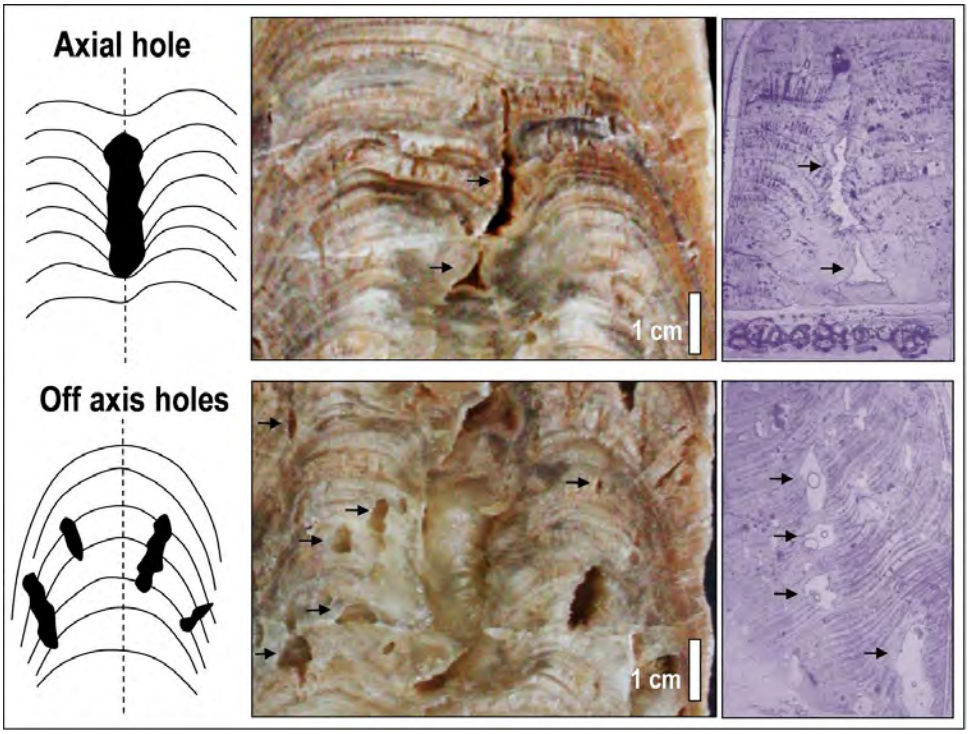

Figure 8. Axial and off-axis macroholes; note the growing layers bending towards the axial holes, and the clear cutting of the growing layers by the off-axis holes, in polished surfaces (middle) or in petrographic thin sections (right).

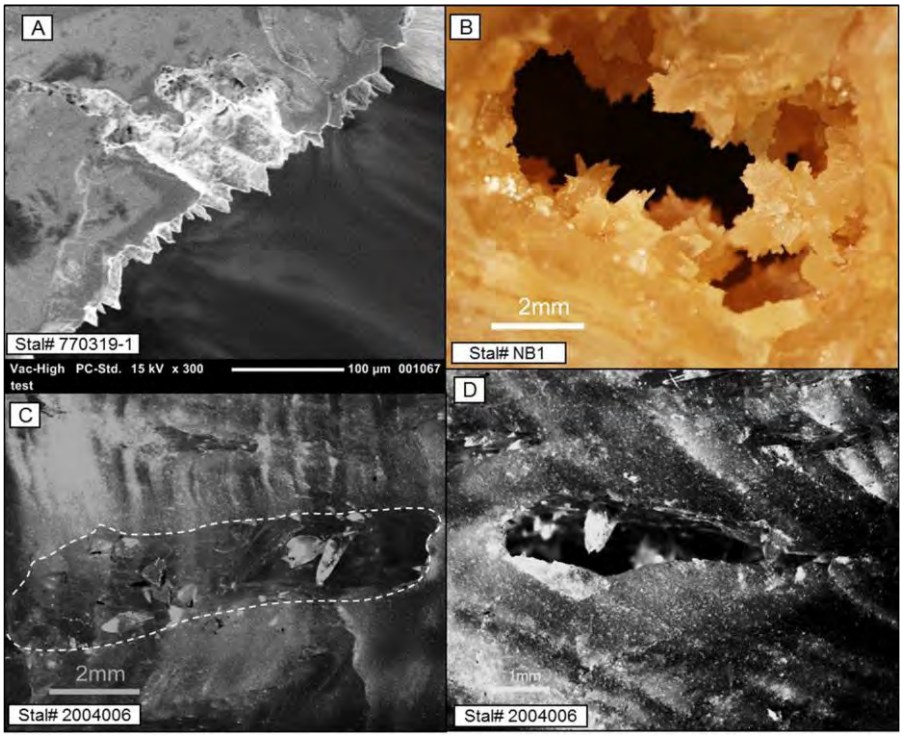

Figure 9. Calcite coatings and new crystals growing epitaxially within off-axis holes. A) SEM imaging; B) new crystals grow to form new coatings along the hole's walls; C and D) no coatings are visible, new crystals grow directly on the holes' substrate. Note the stalagmite growth layers cut by the holes.

According to corrosional and depositional features in macroholes, corrosional features include of spike-like shapes, dissolution thorns or irregular masses of calcite, darker color, and interconnected in places by thin fissures. Depositional features include of calcite film or layers coat the walls of some macroholes (Fig. 9). According to microbial colonization, they found coccoid and filamentous microoranisms (Fig. 10). In addition, classification of macroholes divide into 6 types following the macrohole distributions and architecture in stalagmites. The first one is Intact—none of visible macroholes. Next is Random sparse distribution—randomly distributed and spherical. Holes are non-interconnected. The third one is Axial holes dominant (Fig.8)—axial holes dominated, growth layers bending follow the axial holes. Next is Abundant random holes *("Spongy structure")* —dense surface skin but inner like sponge, elongated parallel to the stalagmites axis, interconnected, and core dissolution. The fifth is Layer-confined holes—usually parallel with growth layers and deposition followed by phase of dissolution activity. This

is the most common types observed. The last one is Mixed type—type 2 and 5 combined and imply corrosional activity.

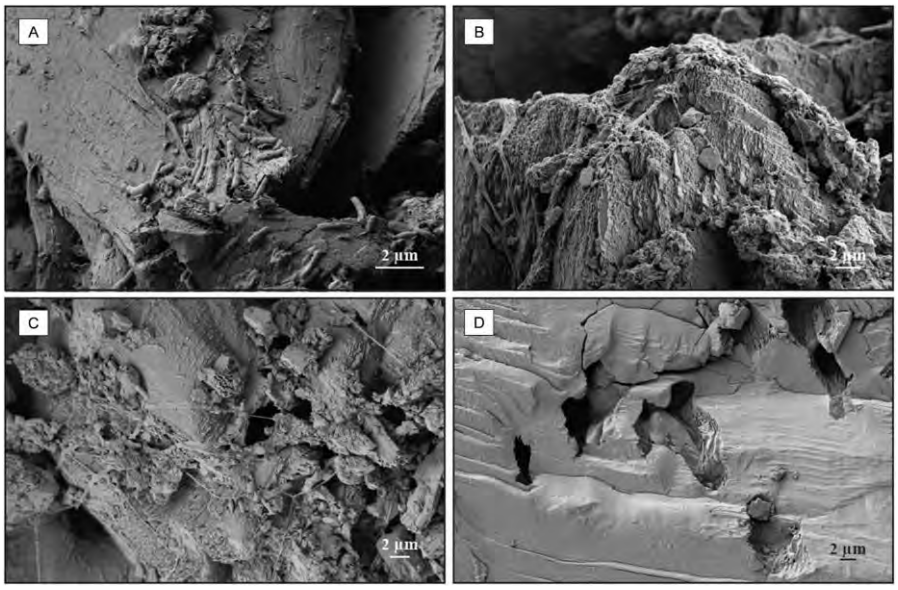

Fig. 10. Secondary Electron Scanning Micrographs of: A) bacteria coating an axial hole surface, forming biofilms along the wall of the axial hole (B); C) organics, fillaments and coccoid cells on an off-axis hole surface (note weathered calcite crystals); D) clean surfaces of calcite within and around micro-inclusions.

Related paleoclimatic study in Thailand:

The latest stalagmites study in Thailand belongs to Muangsong et al., 2014. This study came out from Namjang cave, Pang Ma Pha district, Mae Hong Son province. The study is about physical properties: Grey level and $\delta^{18}O$ of active samples NJ-0901. They measured the age by U-series dating method and the age covered 1901-2008 AD. In addition, they correlated with sample NJ-1 in the same cave from Cai et al., 2010 which the age covered 1901-2005 AD. The results show that amount of rainfall is nearly to each other but slightly different between their growths rates which may cause of complicated climate setting. Besides, they compared the data (Fig.11) with hydrometeorological record at the local meteorology Mae Hong Son station which elapsed 100 years and tried to find the relation of Indian Ocean Dipole (IOD) and El Ni~no-Southern Oscillation (ENSO)

Thailand Monsoon(TM). The results show rarely relationship to each other so that may cause of the climate outside the cave such as raining, aquifer, any processing and environment outside the cave (Fairchild et al., 2006), amount of carbon dioxide during degassing process or climate change abruptly in 1980 AD. Likewise, the relationship between IOD and ENSO with TM are still unclear.

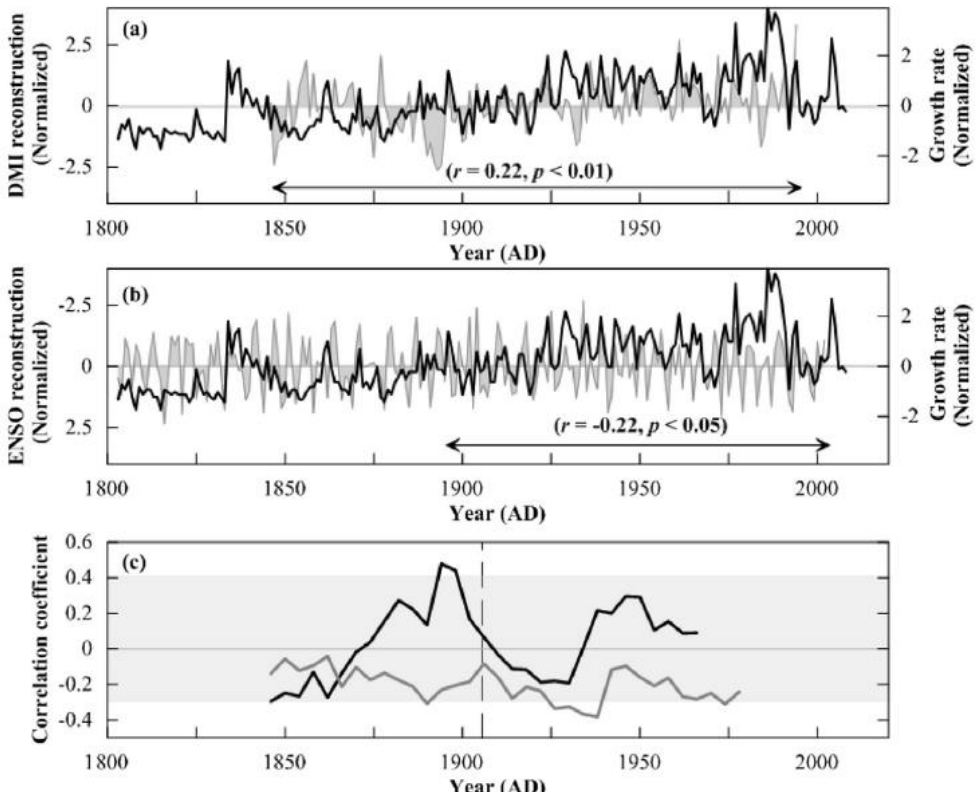

Figure 11. Comparisons of (a) Dipole mode index (DMI) (filled grey line) (Abram et al., 2008), and (b) ENSO (filled grey line; Y axis is reversed) (Li et al., 2011) with NJ-0901 growth rate series (black lines). All data were normalized by their respective standard deviations. Pearson's correlations (r-values) and statistically significant values (bold print) are shown. (c) Thirty-one-year sliding correlation of growth rate with DMI (black line) (Abram et al., 2008) and ENSO (grey line) (Li et al., 2011). 95% confidence levels are indicated using grey bars. The vertical dashed line indicates the boundary at 1905 AD.

Chapter 2

Methodology

The method in this study can be divided into 4 steps as follow.

1. Review related publications.
2. Investigate cave and collect stalagmite samples.
   - Survey for suitable caves (small entrance, less human activity, high humidity, plenty of chambers, deep and long routes).
   - Assesse physical properties of stalagmites e.g., shape color and texture.
   - Collect stalagmite samples (clean, symmetry, absence dissolution texture).
3. Prepare the sample (at department of Geology, Chulalongkorn University).
   - Wash and cut stalagmite samples.
4. Analyze U-Th dating in super clean laboratory at Earth Observatory of Singapore (Nanyang Technological University)
   - Wash the sample with Ultrasonic cleaner.
   - Drill the samples 20 mg. for chemical analysis
   - Chemical preparation for U-Th elements extraction
   - Measurement by quantity of U-Th by multicollector inductively coupled plasma mass spectrometer (MC-ICP-MS)

2.1 Fields Study

- The study area is located in Amphoe Banrai, Uthai Thani province. We investigate caves (16-18 October 2015 and 9-13 January 2016)
- Equipment composes of torch, safety helmet, hammer, and small driller.

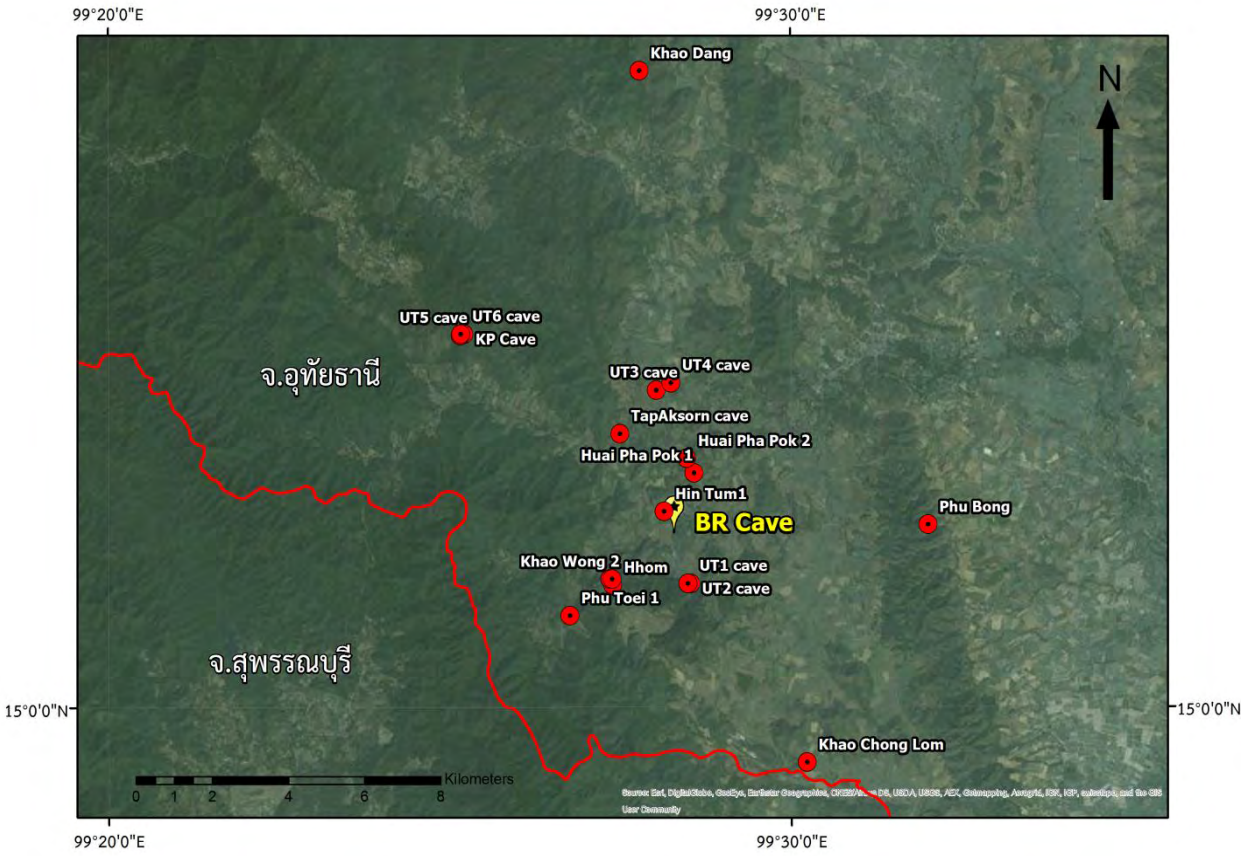

Figure 12. Cave's location (red circle: survey caves; yellow: study site in this study)

Study area	Geographic (Degrees Decimal)		UTM (WGS84)			Elevation(m)
	Latitude	Longitude	Zone	Easting	Northing	
UT1 cave	15.028626°	99.474798°	47P	551038	1661547	236
UT2 cave	15.028579°	99.475439°	47P	551107	1661542	246
UT3 cave	15.073259°	99.467109°	47P	550201	1666482	191
UT4 cave	15.074951°	99.470667°	47P	550583	1666670	230
UT5 cave	15.085974°	99.419261°	47P	545056	1667878	385
UT6 cave	15.086281°	99.419327°	47P	545036	1667856	396
Khao Prae cave	15.086279°	99.420155°	47P	545152	1667912	447
TT cave	14.573559°	101.148520°	47P	731418	1612253	n/a
Tap Aksorn cave	15.063224°	99.458192°	47P	549245	1665370	244
Ban Rai cave	15.052225°	99.482414°	47P	551851	1664159	203
Hin Tum1 cave	15.045165°	99.468945°	47P	550405	1663375	421
Phu Toei 1 cave	15.021189°	99.445953°	47P	547939	1660718	326
Khao Dang cave	15.147059°	99.463072°	47P	549750	1674644	397
Huai Pha Pok 1 cave	15.054028°	99.476333°	47P	551197	1664357	310
Huai Pha Pok 2 cave	15.057467°	99.474517°	47P	0551001	1664737	206
Hhom cave	15.028203°	99.456396°	47P	0549060	1661496	323
Khao Wong 1 cave	15.029632°	99.455692°	47P	548984	1661654	331
Khao Wong 2 cave	15.028049°	99.456209°	47P	549040	1661479	337
Khao Chong Lom cave	14.987192°	99.503808°	47P	554167	1656971	256
Phu Bong cave	14.974386°	99.533455°	47P	557358	1655562	276

Table.1 Grid location of caves.

➢ Collecting sample

This process based on basic physical properties of stalagmite–color, texture, and shape. In this study, we collect three samples, two broken samples (BR1 and BR2) and one standing stalagmite (BR3). To conserve the natural resource. Our sample collected at BR cave (see location in Fig.12).

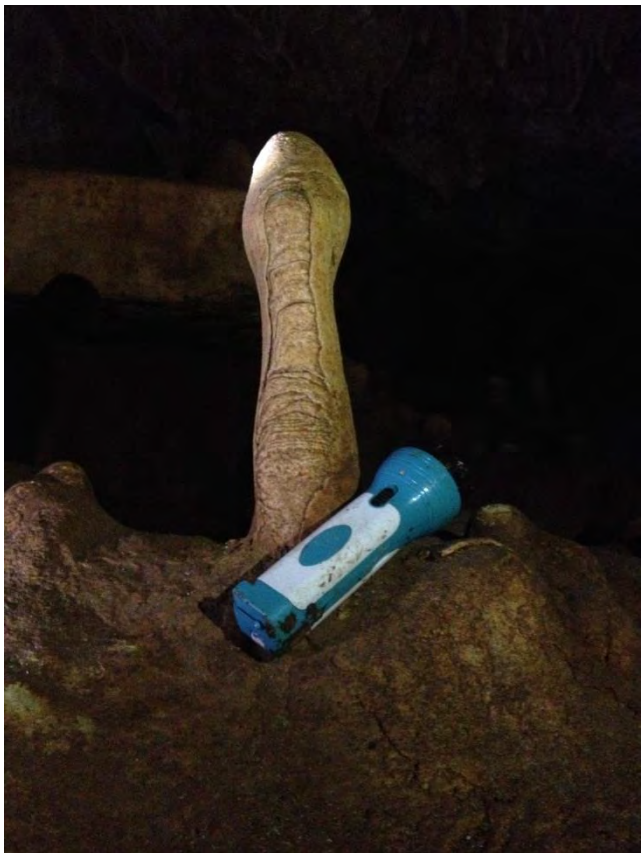

Figure 13. Standing sample (BR3)

2.2 Preparing samples

At Department of Geology, Chulalongkorn University, we washed samples and cut them by saw blades (with oil) along longitudinal axis to separate them into 2 pieces (Fig.15-17)

Figure 14. Samples before cutting

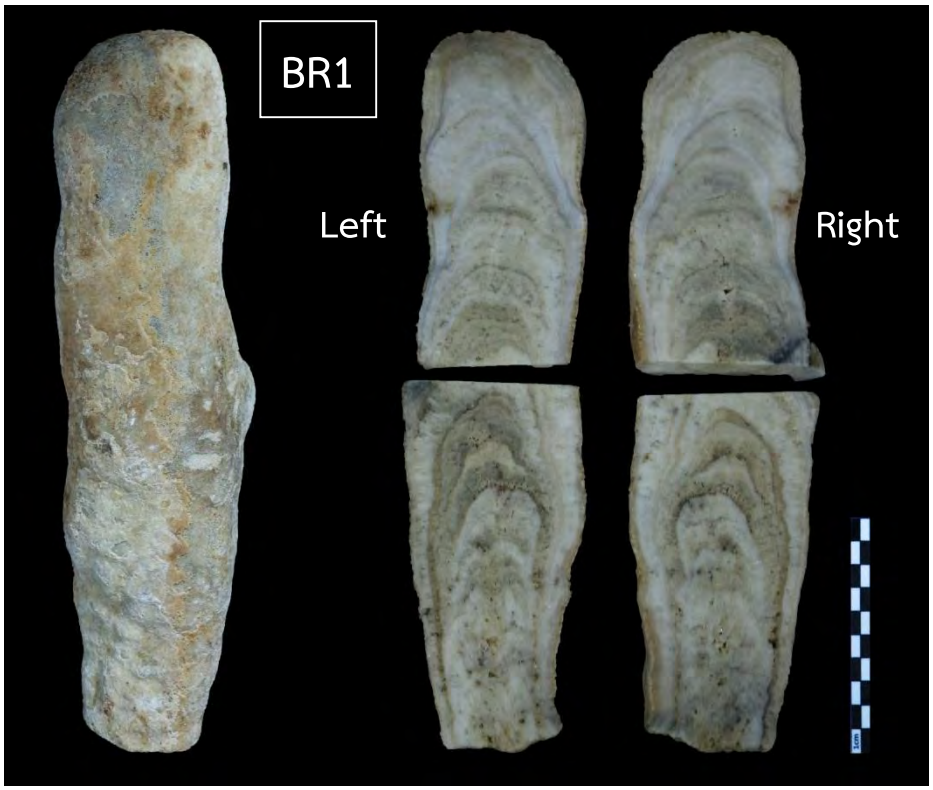

Figure 15. BR1 sample.

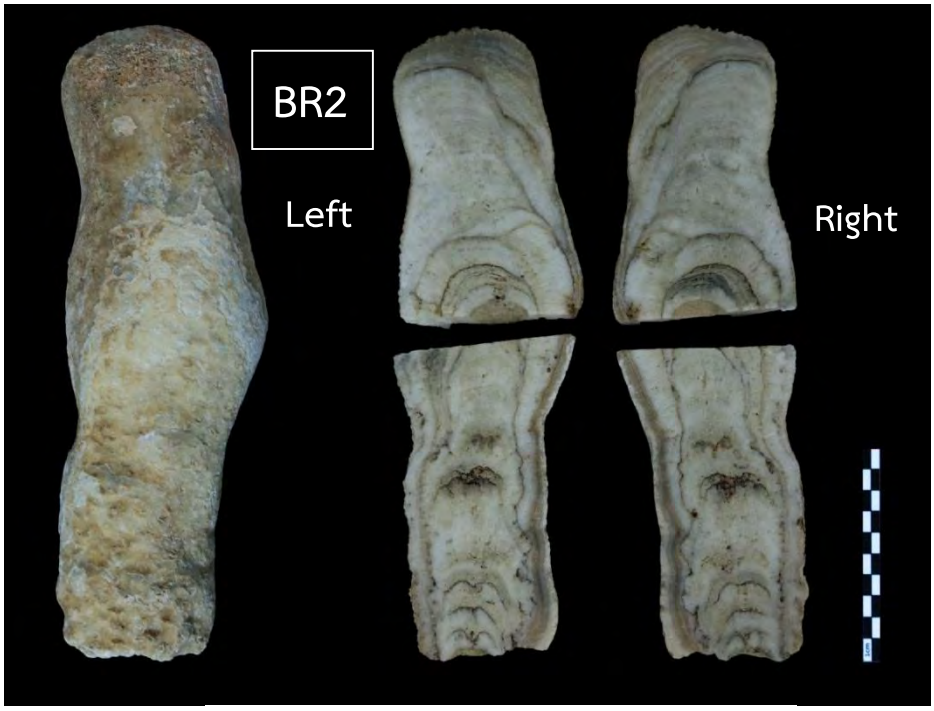

Figure 16. BR2 sample.

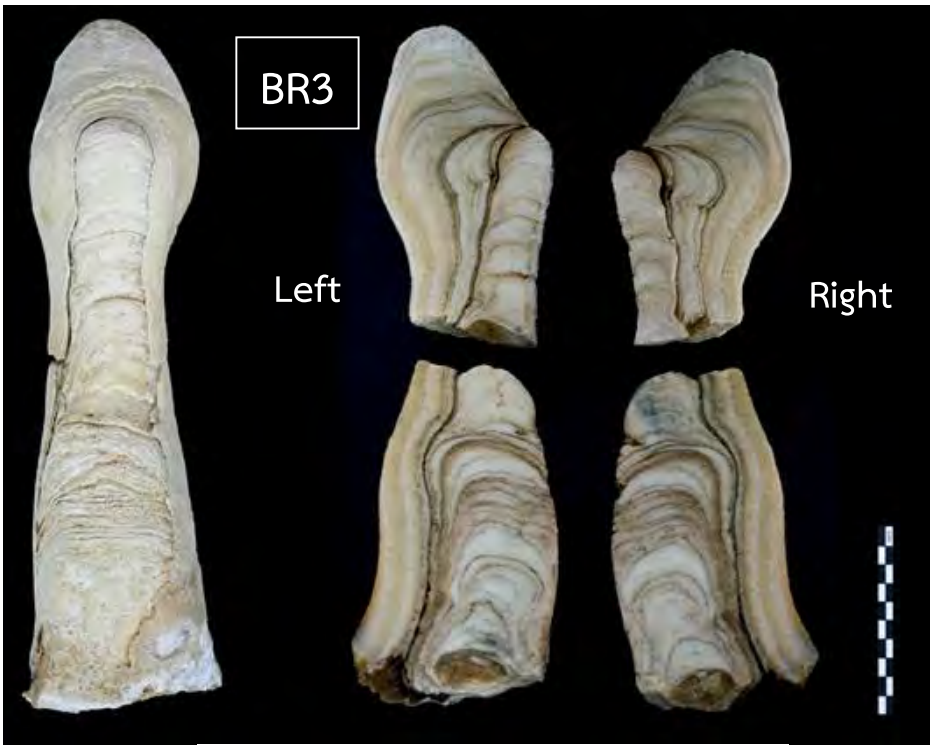

Figure 17. BR3 sample.

2.3 Laboratory at Earth Observatory of Singapore

➢ Wash samples with Ultrasonic Cleaner

1. Take samples in Ultrasonic cleaner with normal water. Use the frequency at 53 KHz and temperature at 20°c around 20 minutes.
2. Take the water and samples out to wash the cleaner. Then, change the water into Deionized water. Do it twice.
3. Dry the sample in sampling room for 1 day.

Figure 18. Washing sample in Ultrasonic cleaner machine with Deionized water.

➢ Drilling

1. Place the clean wipes on the working bench for the clean surface.
2. Put a clean drill bit in the dentist's drill and tighten (0.5-0.7 mm for U-Th dating samples)
3. Put on new gloves
4. Take out a new piece of weighing paper which you will put the powder on.
5. Select the growth layer on sample where you would like to drill.
    - Scratch the select layer first and should drill near the central axis.
    - Drill perpendicularly with target.
    - Drill along the growth layer (not too deep) and do not drill across the growth layer.
6. Clean the vial by air gun.
7. Transfer the powder to the vial.
8. Use the air gun to get rid of remained powder.
9. Weigh the vial to 20 mg (for 2-5 ppm U conc.).
10. Cap and label the vial.
11. Start the next drill.
    - Clean the drill bit by acid (HCl conc.) and methanol, respectively.
    - Change weighing paper.
12. Repeat steps 5-10.
13. Put all the samples to Ziploc for transferring.
14. When finished, turn off the drill and discard the drill bit you used
15. Close the laminar flow bench and clean up anything else that needs it

Figure 19. Drilling must only do in Air clean hood.

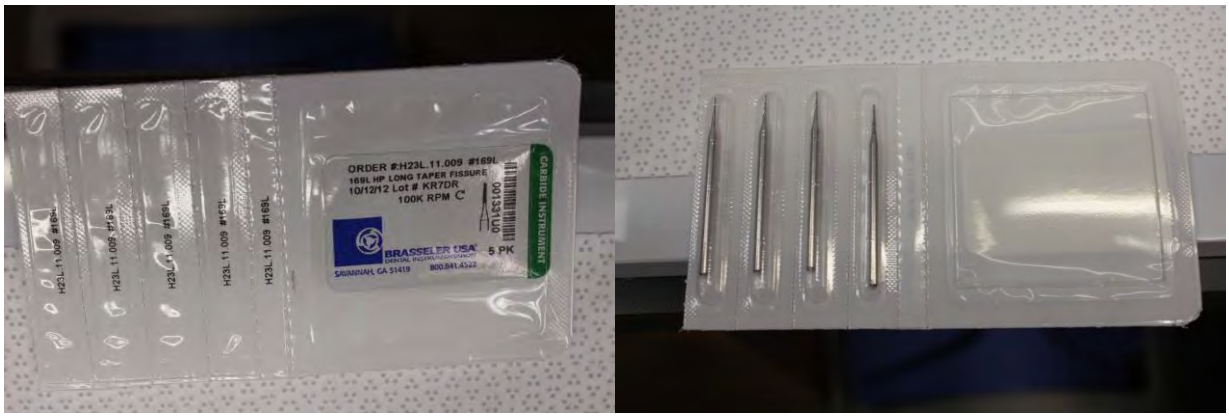

Figure 20. Drilling heads.

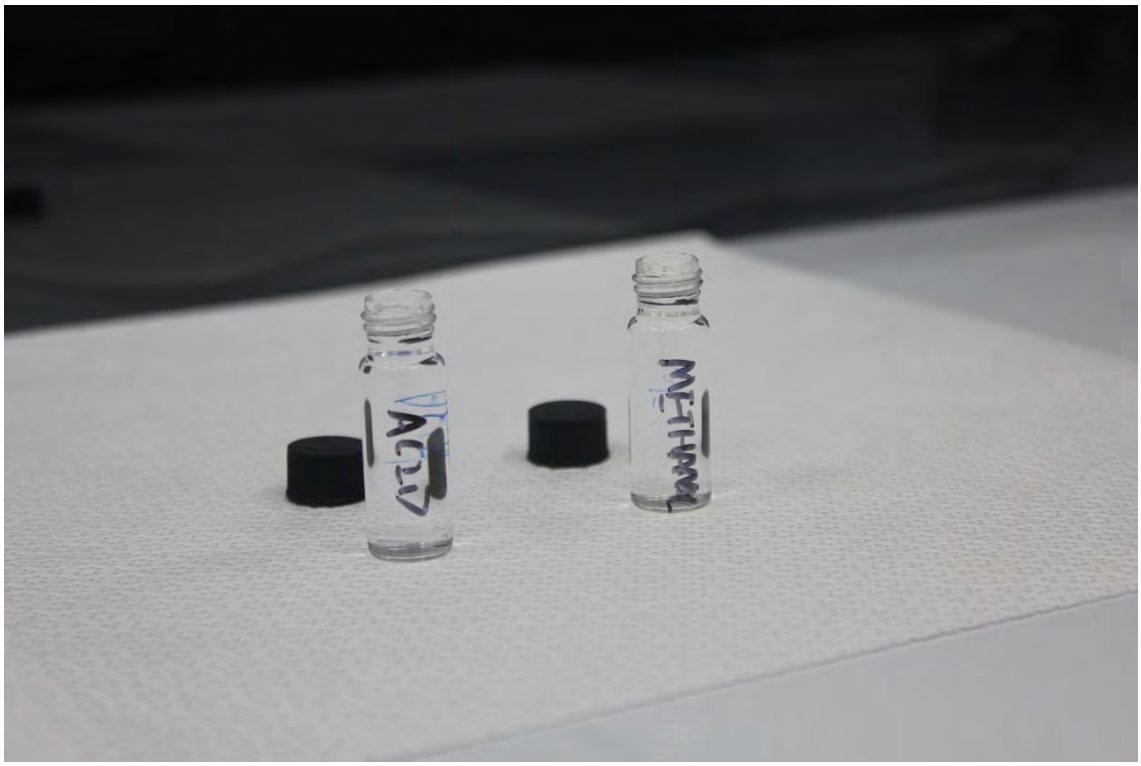

Figure 21. Acid and Methanol for wash drilling head.

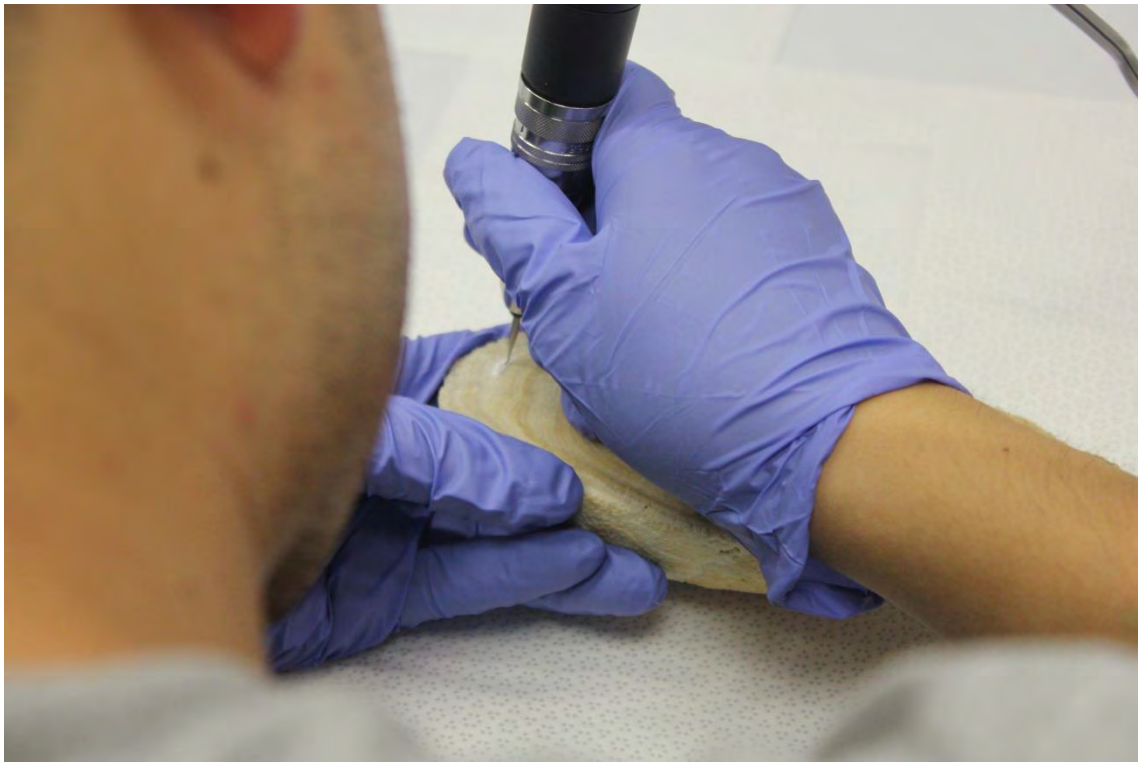

Figure 22. Drilling sample.

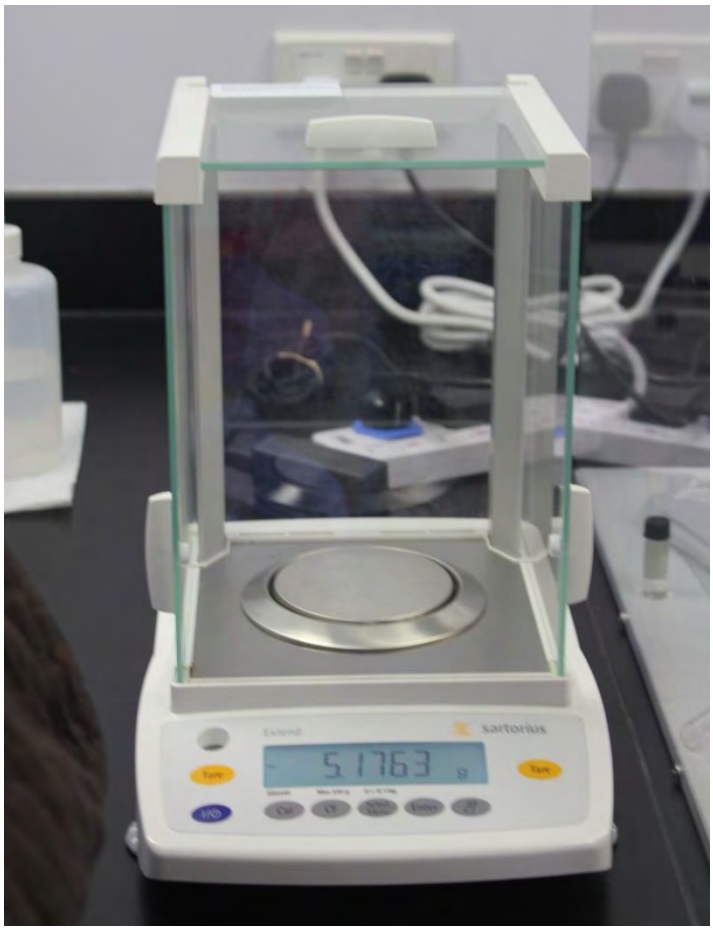

Figure 23. Scientifc balance.

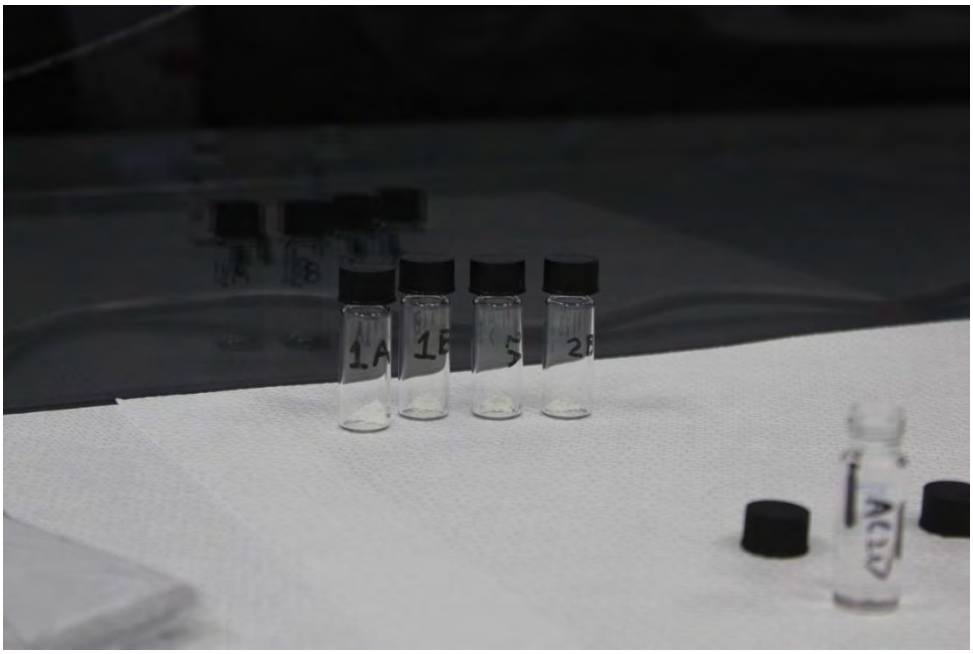

Figure 24. Vials for powder samples.

Figure 25. Atmosphere in sampling room.

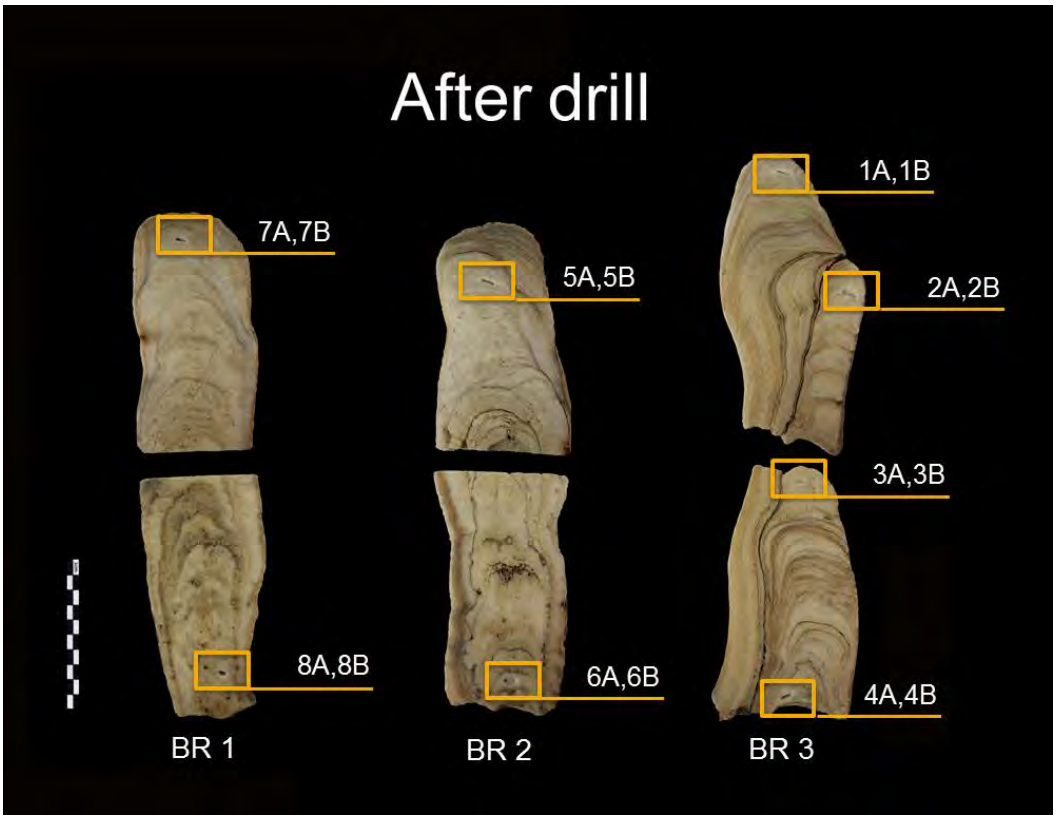

Figure 26. Position of drilling.

➢ Chemistry

Attention !!

- Do it all in chemical fume hood except centrifuge steps.
- If it's a powder sample, you must weight it before adding spike (calculate in measurement).
- If you see something wrong, tell the advisor immediately.

Blank preparation.

1. Prepare Teflon beakers
2. Rinse H_2O + $7N\ HNO_3$
3. Weight and tare the samples (record).
4. Pipet 10 μl of spike
5. Weight spike (record).
6. Add $14N\ HClO_4$ for 2 drops.
7. Reflux with hotplate at 180°c for 2 hours.
8. Rinse H_2O + $6N\ HCL$ + cap

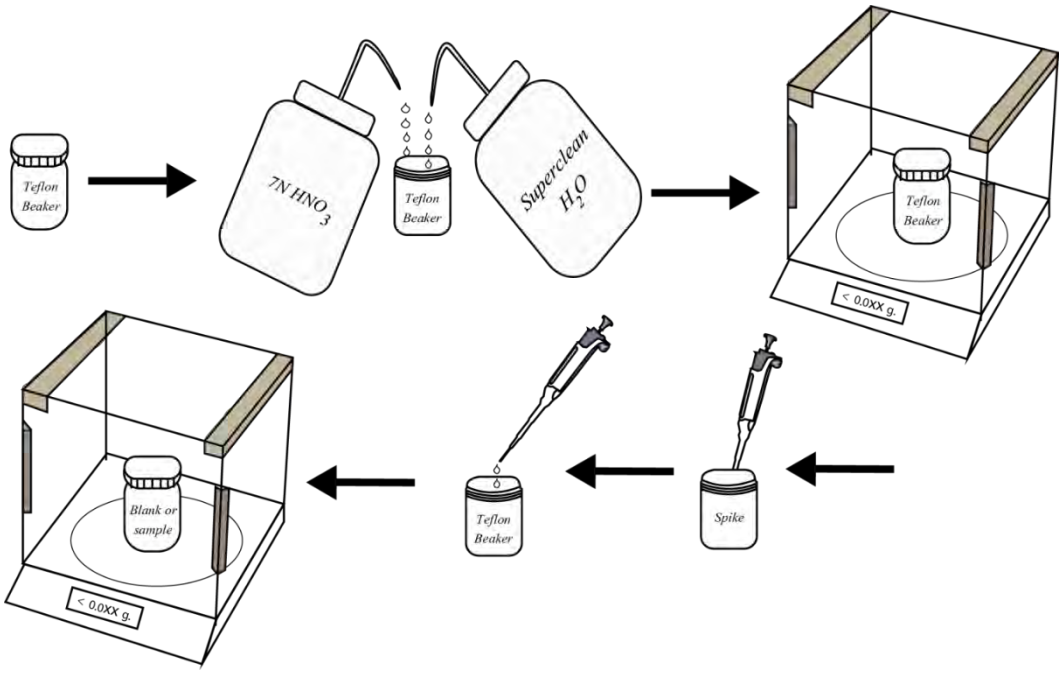

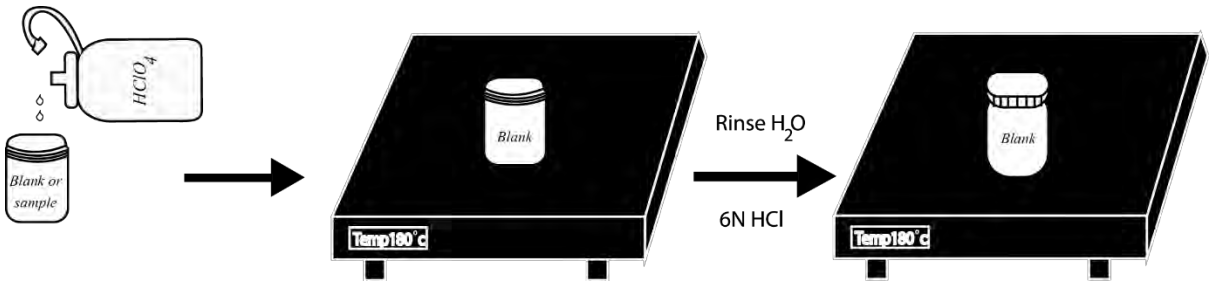

HNO_3 for dissolve
$HClO_4$ for get rid of organic matter
HCL for dissolve and get rid of metal, alloy, and ores

Iron Co-Precipitation Procedures (Before the centrifuges)

1. Transfer to centrifuge tubes. Then, let the beakers dry down with $7N\ HNO_3$
2. Add 3 drops of $FeCl_3$ (drops depend on acidity of samples)
3. Titrate with NH_4OH (around 3 drops) until the color changes to yellow (a little bit orange-precipitated $Fe(OH)_3$)
4. Add super clean water around $^2/_3$ of tube with weight balance of opposite site must not more than 0.004 g and cap with cleaned parafilm.
5. Centrifuge with 2500 rpm (around 8 minutes)
6. Only pour off the supernate and repeat step 4-6 for 3 times.
7. Place the tube in a rack.

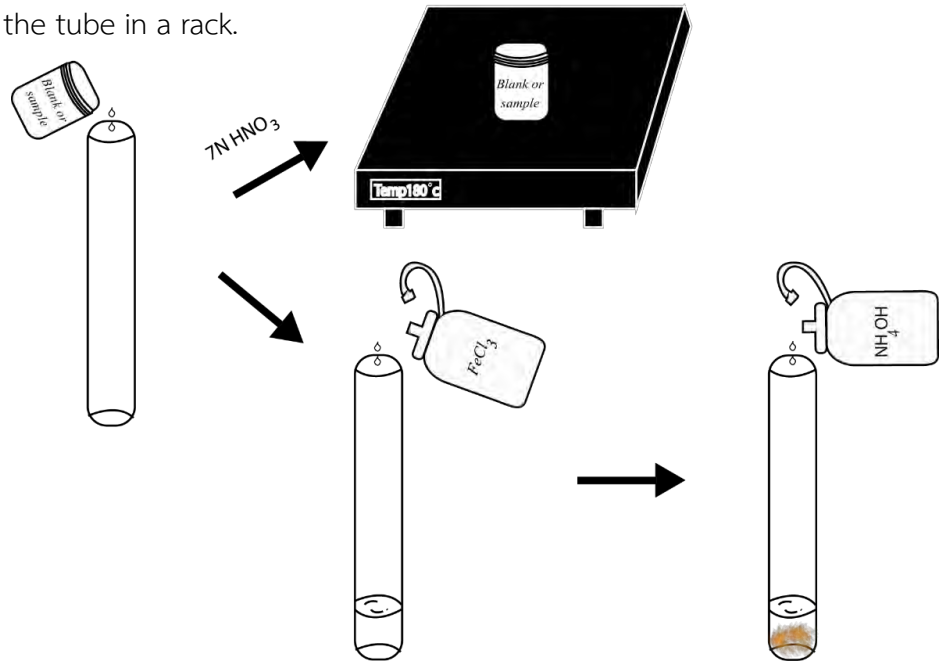

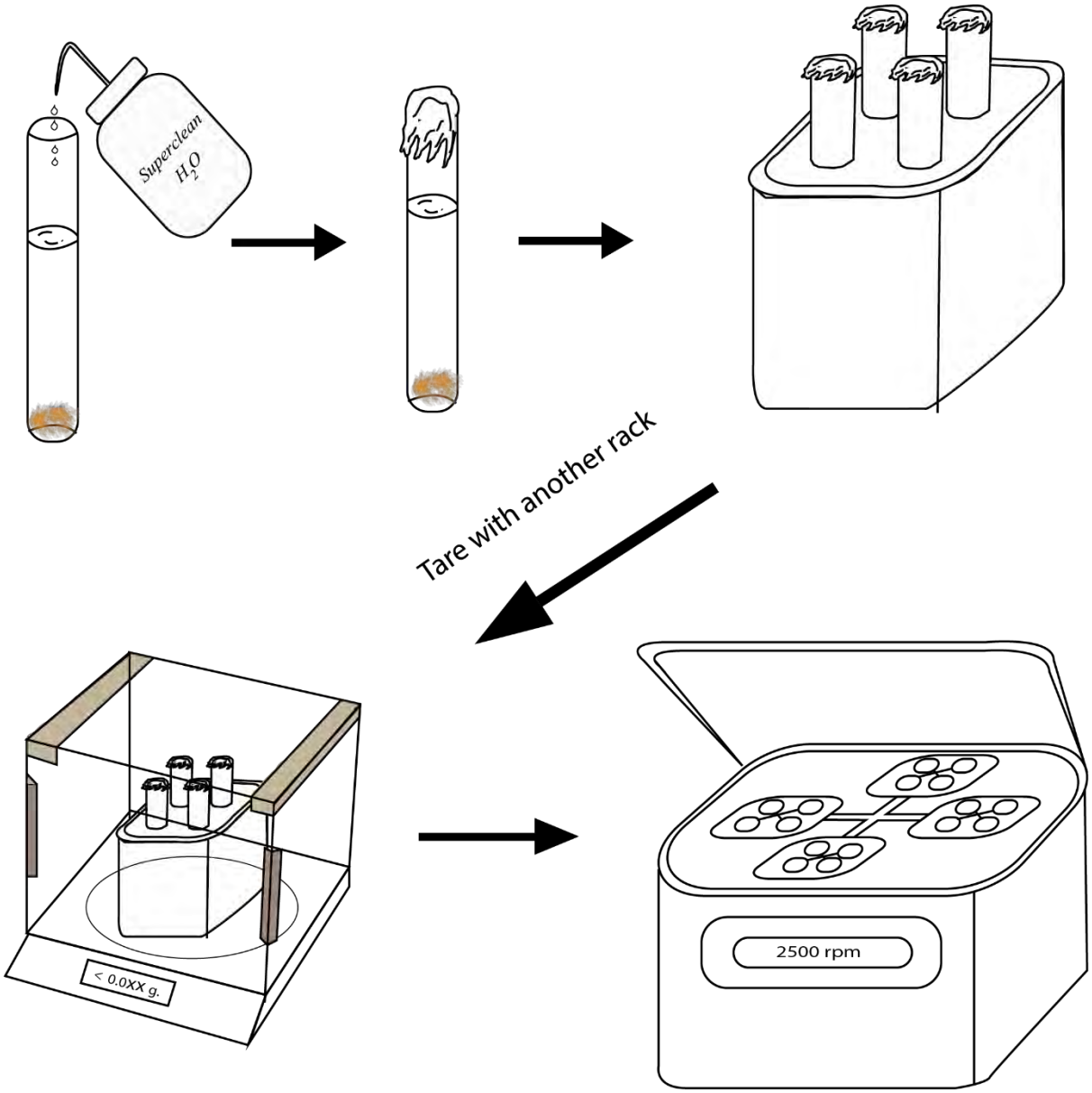

$FeCl_3$ will react with NH_4OH. As a result, we will get $Fe(OH)_3$ (s) and $CaCl_2$ (l).

After these steps we will get rid of Fe by Column

Preparing Columns (During the centrifuges)

1. Wisely choose a column
2. Put Fritz (filter that only water can pass) to each column
3. Punt columns in holder and place Pyrex beaker under each column to collect chemical waste.
4. Fill each column with super clean water and full of water (no bubbles). Keep them full all the times.
5. Pipet clean resin into each column to the neck of column.

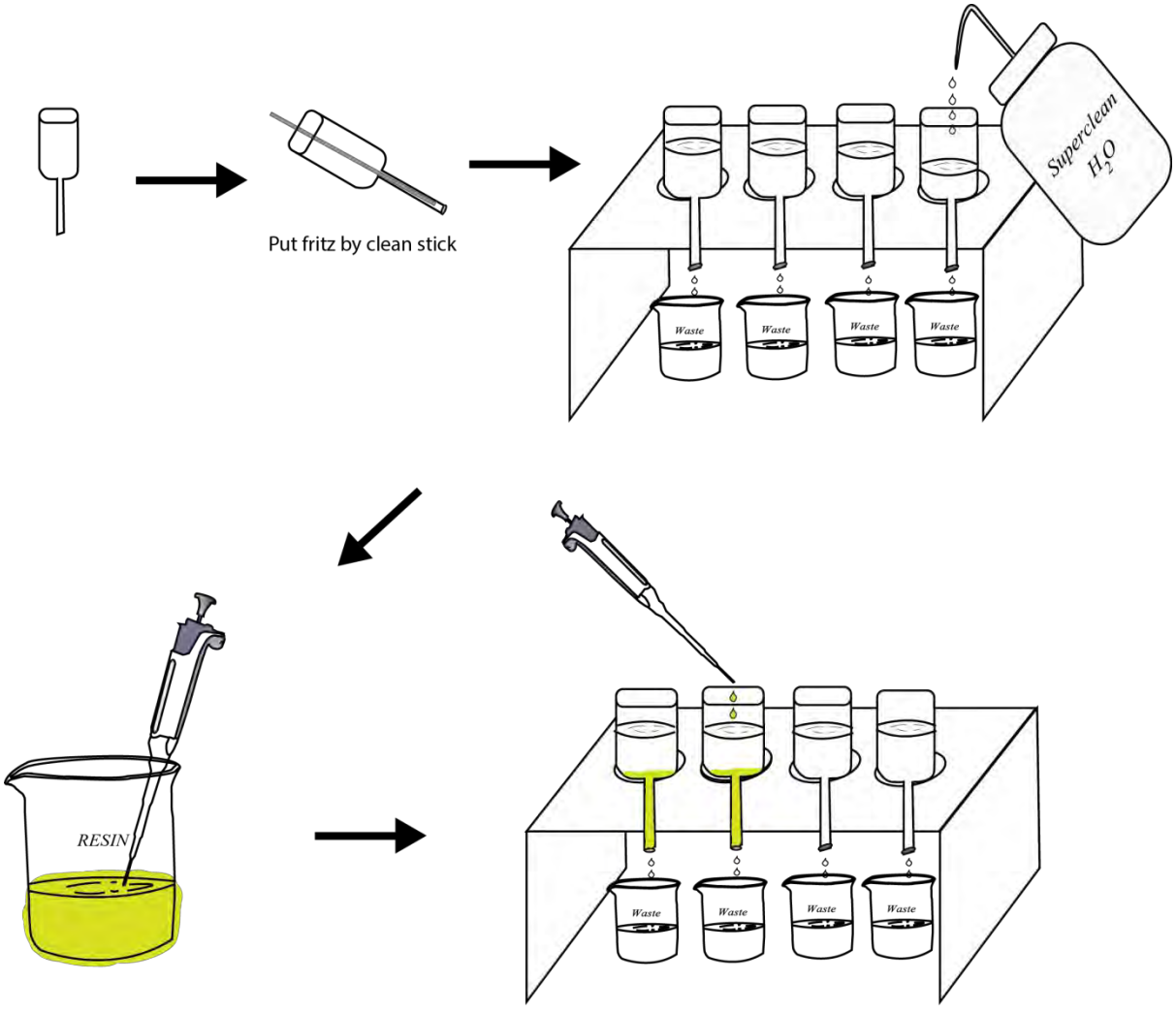

Preconditioning

- Add 1 drop of $14N\ HNO_3$ (full of water) for clean the resin.

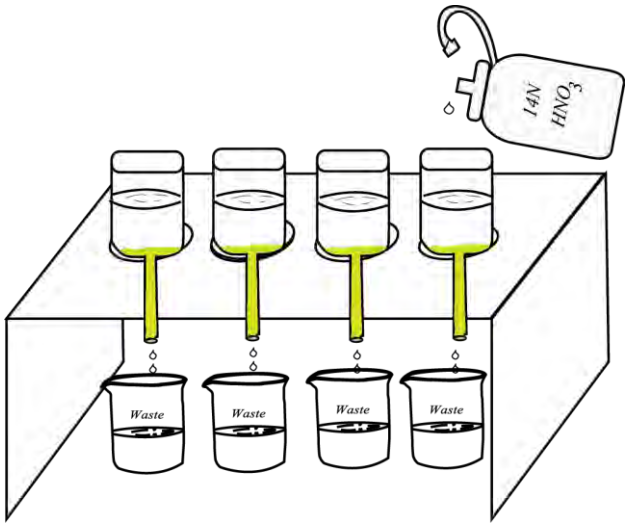

Iron Co-Precipitation Procedures (After the centrifuges)

1. Add 10 drops of $14N\ HNO_3$ to centrifuge tubes to dissolve. Then, pour back to the beakers.
2. Add 1 drop of $14N\ HClO_4$ and dry down.
3. Add 1 drop of $14N\ HNO_3$ and dry down (HNO_3 environment).
4. Rinse $7N\ HNO_3$ to each beaker to re-dissolve.
5. Load the samples to each column. Then, keep the beakers reflux.

Conditioning

- Add 1 drop of $14N\ HNO_3$ to each beaker.
- Add 2 CV $7N\ HNO_3$ to each column
- Add 1 CV $7N\ HNO_3$ to each column

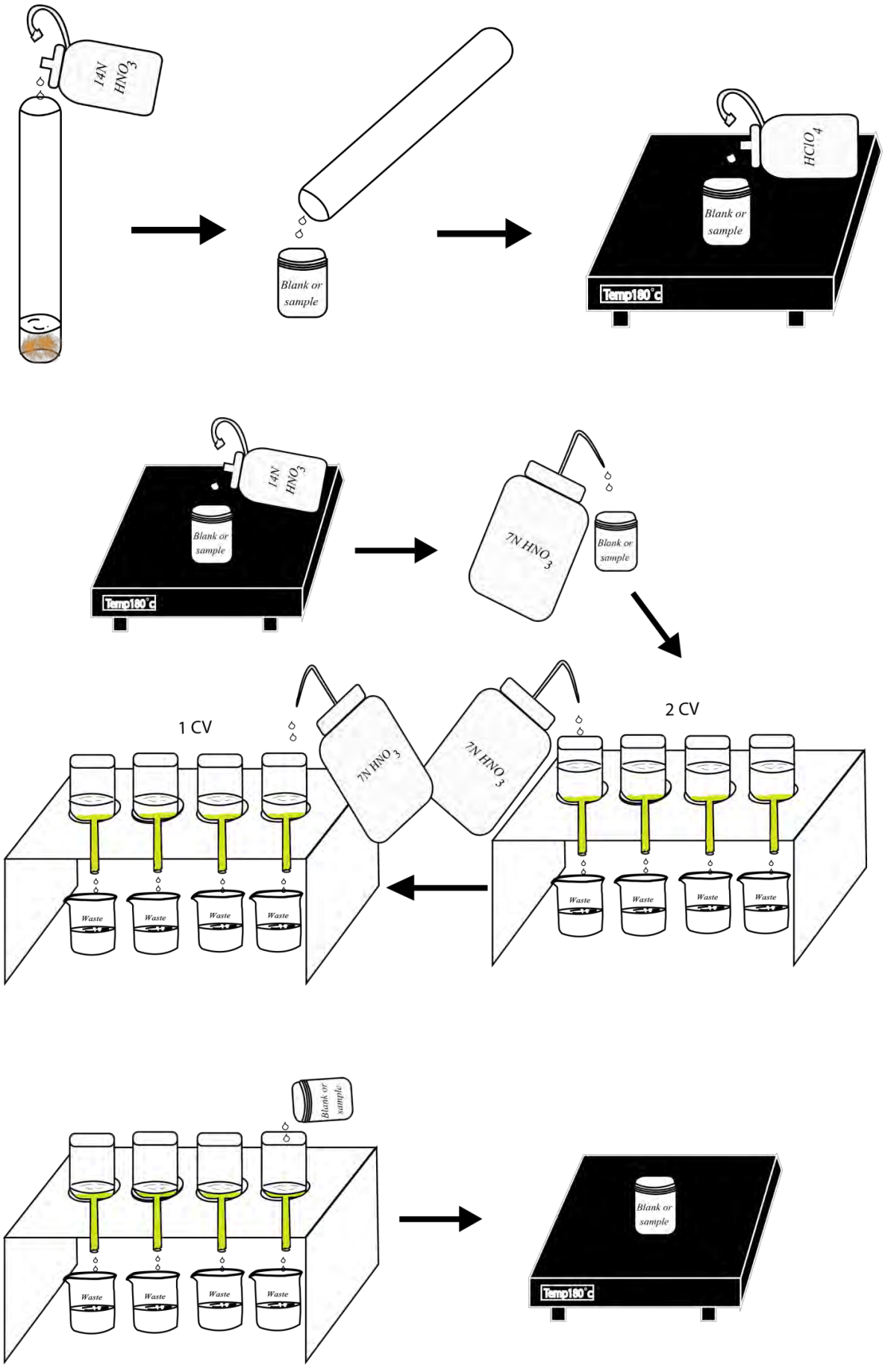
14N HNO3
Blank or sample
HClO4
Blank or sample
Temp180°c
14N HNO3
Blank or sample
Temp180°c
7N HNO3
Blank or sample
1 CV
7N HNO3
7N HNO3
2 CV
Waste
Waste
Waste
Waste
Waste
Waste
Waste
Waste
Blank or sample
Blank or sample
Temp180°c

Column Chemistry

Remove Fe

1. Add 2 CV $\mathbf{7N\ HNO_3}$ to each column.
2. Add 1 CV $\mathbf{7N\ HNO_3}$ to each column.
3. Remove waste beakers.

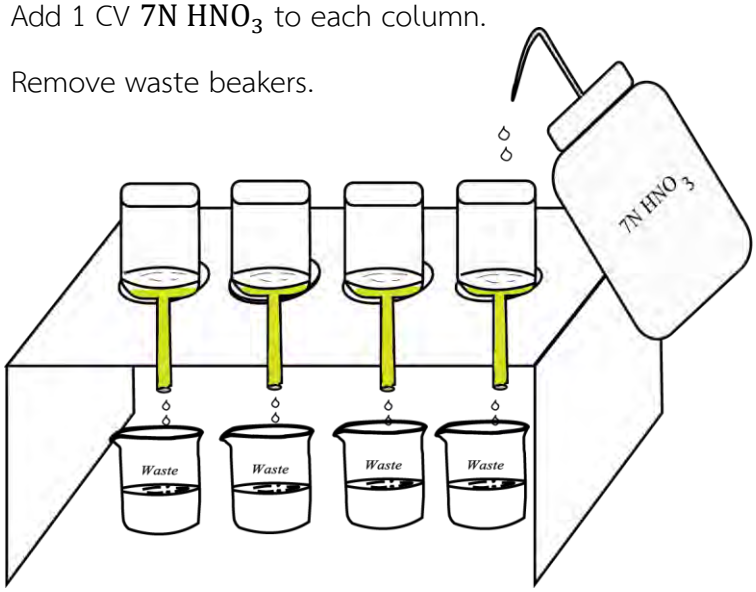

2 CV and1 CV respectively.

Collect Thorium

1. Place the new small Teflon beakers
2. Add 2 CV $\mathbf{6N\ HCl}$ to each column.
3. Add 1 CV $\mathbf{6N\ HCl}$ to each column.
4. Remove beakers and add 1 drop of $\mathbf{HClO_4}$.
5. Dry down on hot plate.

2 CV and1 CV respectively.

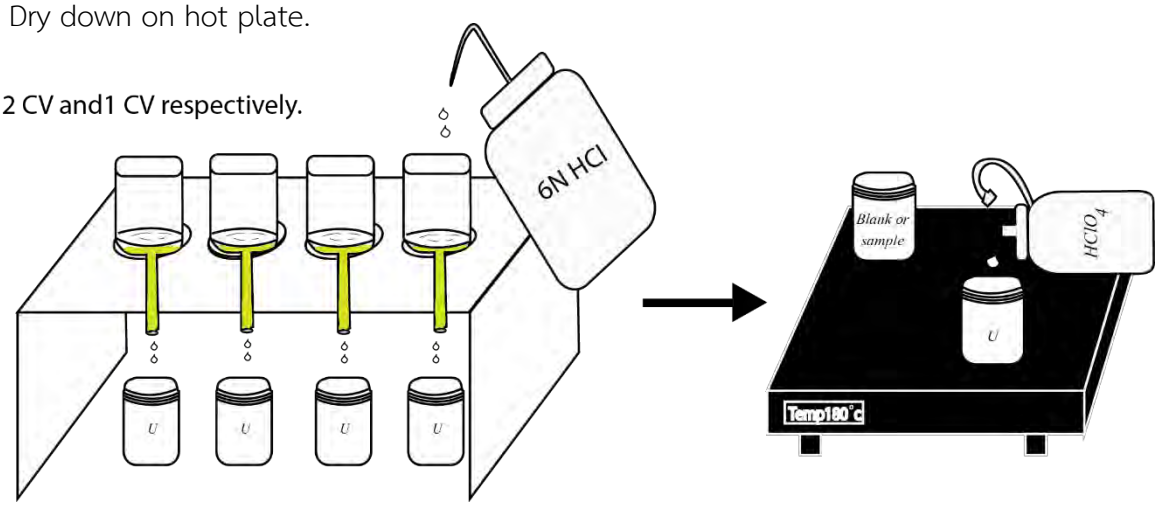

Collect Uranium

1. Place the refluxed beakers instead.
2. Add 2 CV H_2O to each column.
3. Add 2 CV H_2O to each column.
4. Remove beakers and add 1 drop of $HClO_4$.
5. Dry down on hot plate.

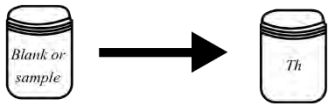

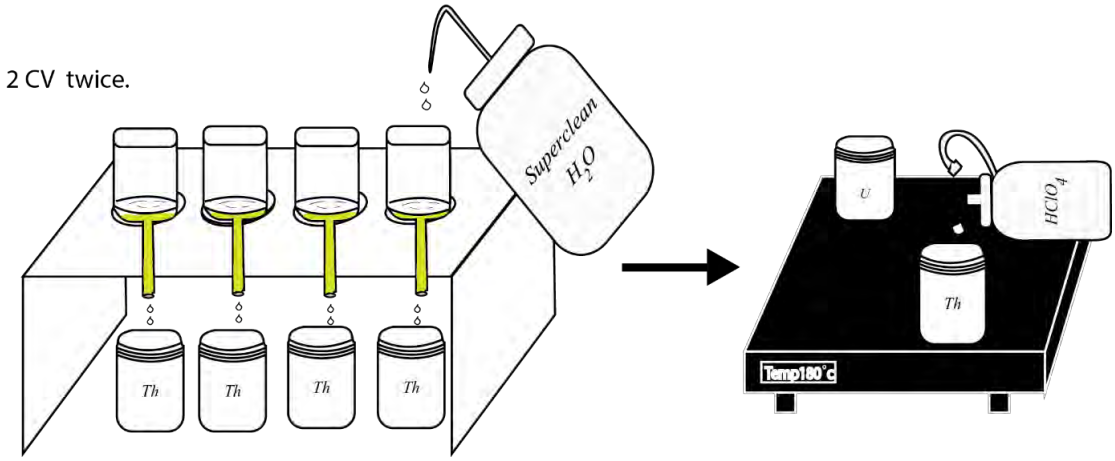

Preparing ICP vial storage

1. Add 1 drop of $HClO_4$ to each beaker and dry down.
2. Add 1 drop of $14N\ HNO_3$ to each beaker and dry down.
3. Add 1 drop of $14N\ HNO_3$ to each beaker and **dry nearly complete**.
4. Add ICP-solution immediately.
5. Transfer to vials.

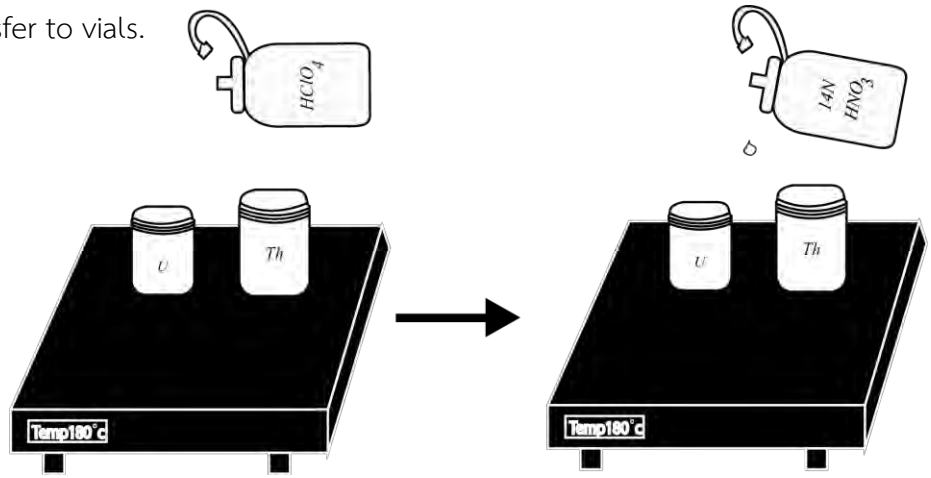

Figure 27. Chemistry room.

Figure 28. Chemistry room.

➢ Measurement by multicollector inductively coupled plasma mass spectrometer (MC-ICP-MS)

1. Check every machine to ready to start. (By Staff)
2. Open the program, TUNE- [Neptune], which connected with MC-ICP-MS machine.
3. Bring the vial to lab
4. Start the measurement with ICP-solution first to recheck the machine.
5. Measure vial. If amplitude signal of graph that shows in monitor screen is higher than 0.005 mV, dilute it.
6. Let cycle running around 500 cycles, stop and save data
7. Back to measure ICP-solution again and do every time before measure the next vial.(Recheck the machine)
8. When finished, turned every machine off. (By Staff)
9. Take data to calculate age in Microsoft Excel program that already have function for calculate. (By staff)

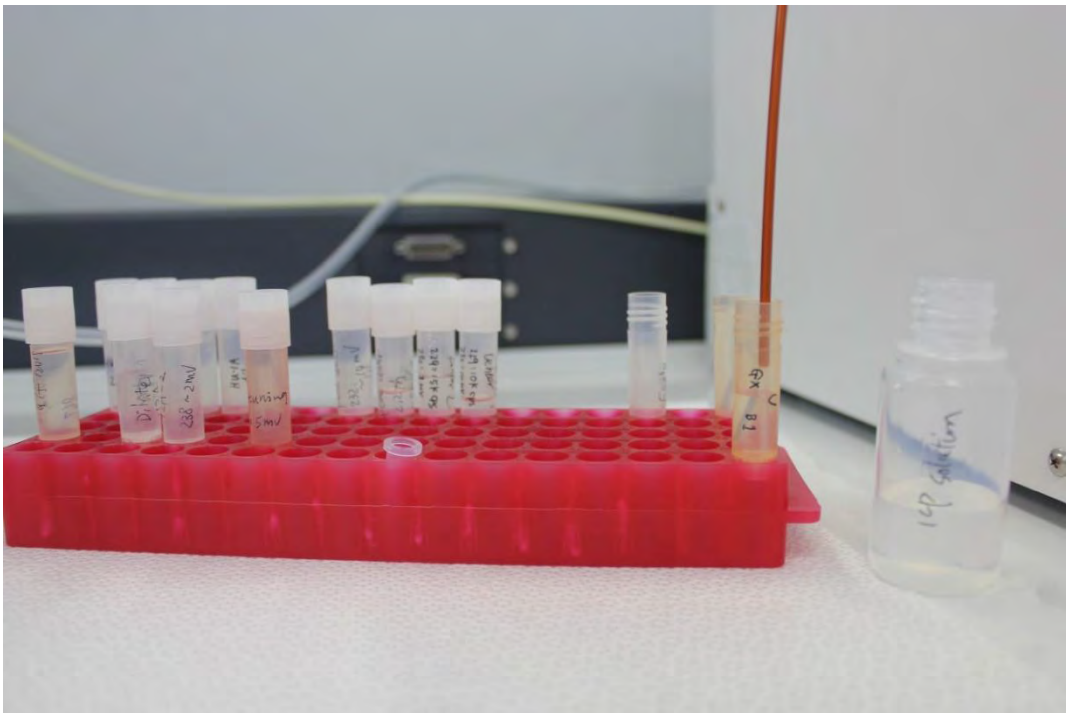

Figure 29. Vial test.

Chapter 3

Results

3.1 Physical properties assessment

In the field survey, we determined the outer properties of stalagmites to ensure that the sample has a potential and useful for paleoclimatic study. Because U-Th dating method is quite expensive, the sample must be worth to risking for. However, we prefer to collect the broken samples than standing (living) one to test according to the concern about natural reserve.

***BR1*:** This sample is cut into 4 pieces by rock cutting machine (with oil) at Department of Geology, Chulalongkorn University. We assessed the shape and surface skin on Figure30a. Samples BR1 has length 31 cm. and the diameter ranges between 6 and 8cm. The shape looks nearly symmetrical candle shape. But the surface shows corrosion features— rough skins, and visible macroholes (Shtober-Zisu et al., 2014).

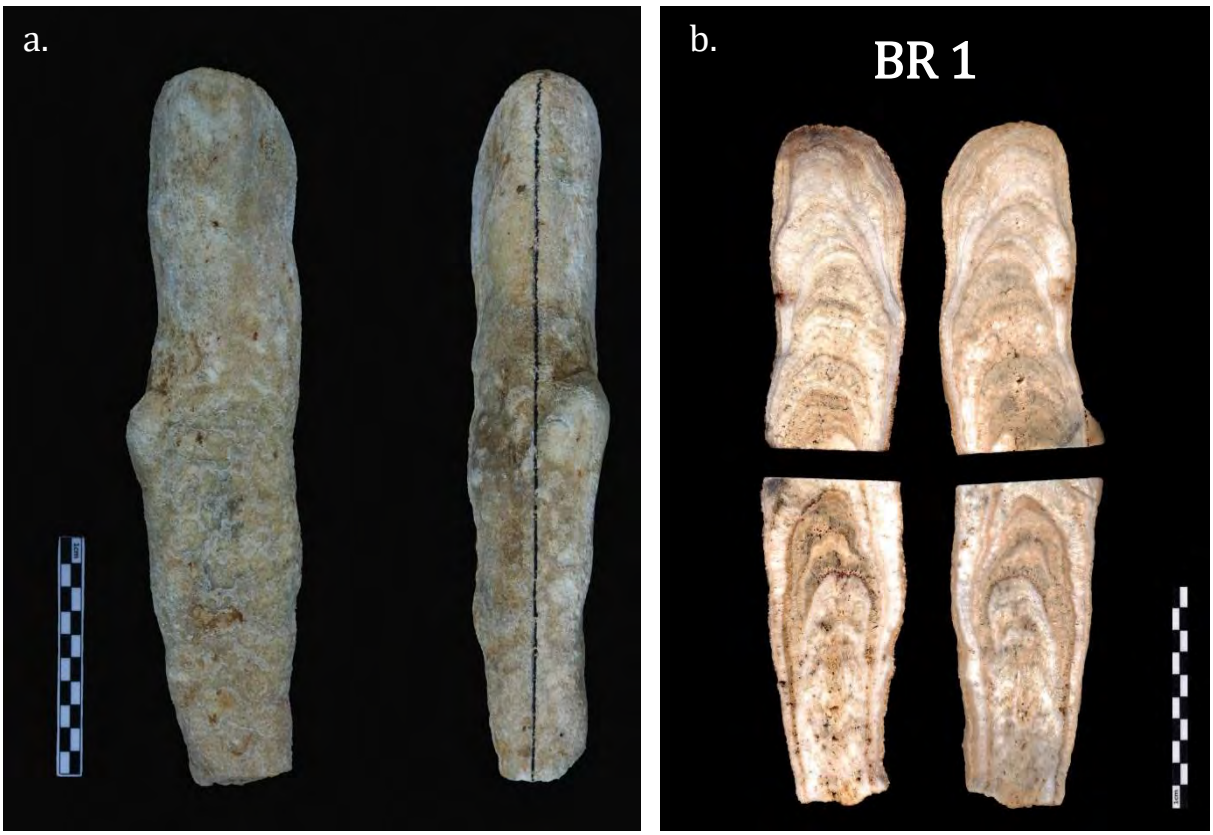

Figure 30 (a.) Surface skin of BR1 sample and linear of longitudinal section for cutting. (b.) scanned cut-samples show inner skin, texture, and color of growth layers.

Figure 31. Drilling positon of BR 1.

Fig 32. Drilling positon of BR 2 sample.

The surface color is greyish yellow, weathered color of calcite. After cutting process towards to Figure 30b. which shows the inner, there are many small cavities and seem discontinuity. The growth layers are shifted from the middle of the upper part (Fig.31). According to the layer colors, the lighter color is chosen for a drilling point than darker color. The darker color layer of stalagmite might be precipitated in unclosed system. Thus, we prefer to choose the lighter band for dating process. According to Figure 31, shows the drilling position on the top and bottom according to the age range of stalagmite precipitation.

***BR2*:** has the length 28 cm and diameter of 8-10 cm. (Fig 33). The shape looks nearly symmetrical candle shape with larger diameter in the middle part which may cause by shifting the position of dripping water. The surface texture is more irregular and rougher than BR 1 sample. Corrosion features show like BR 1, rough skins and visible macroholes. The surface color shows weathered greyish yellow color like BR 1 sample. On the Figure 33b, the inner skins shows different colors. The growth layers shows lighter colors than BR1 sample but still have an interfingered

darker band with lighter band. Besides, there are a discontinuity layer that seem like a hiatus on the upper part and a few on the lower part. This may cause by shifting drip water pattern. In this sample, we choose the lighter band before the discontinuity layer as the top and bottom of sample for dating process (Fig.32).

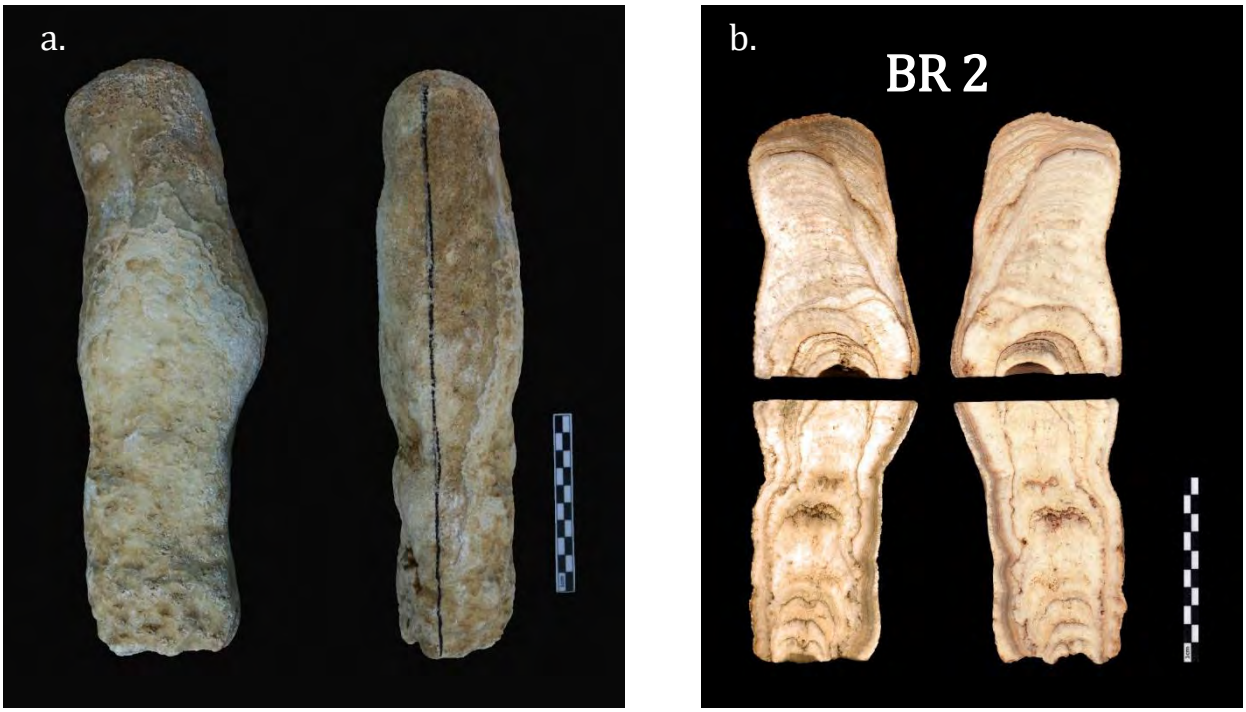

Figure 33 (a.) Surface skin of BR2 sample and linear of longitudinal section (b.) Scanned cut-samples show inner skin, texture, and color of growth layers.

***BR3*:** is quite different from BR1 and BR2 samples. The BR 3 sample has a little one inside (stalagmite in stalagmite; Fig.34). The length of outer stalagmite is 36 cm. and the diameter of 8-11 cm. The length of inner stalagmite is 26 cm. and the diameter of 3-6 cm. This is the only one standing sample that we broke from the BR cave. Both stalagmites has a symmetry shape as well but the surface shows the corrosion texture which make them very low potential for dating method. The surface color of both stalagmite are lighter than the others sample. The inner stalagmite composes many darker growth layers and growth axis is unlike the outer stalagmite (Fig.34b). The inner

Figure 34 (a.) Surface skin of BR3 sample and linear of longitudinal section which was cut. Photo was taken by camera. (b.) cut-samples show inner skin, texture, and color of growth layers. Photo was scanned by printer.

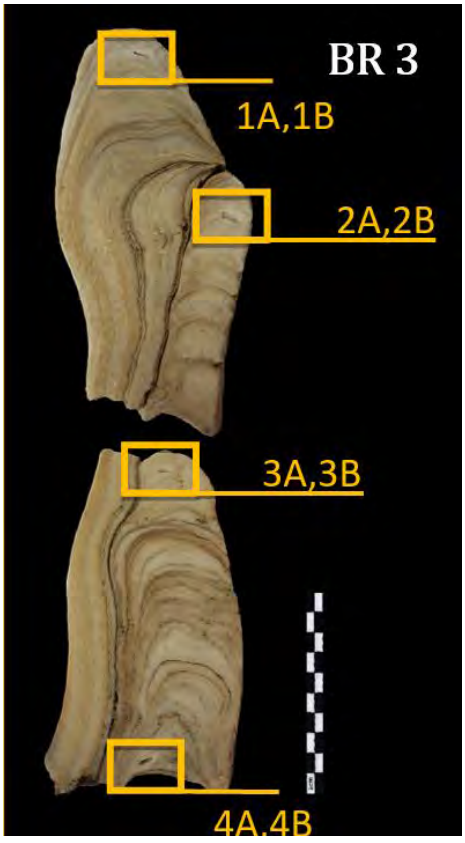

Figure 35. Drilling positon of BR 3.

stalagmite connected with outer stalagmite by discontinuity layer. So we infer that the inner and outer stalagmite was precipitated in different events ostensibly. In addition, there are some darker layers interpolated in growth layers but in a good orientation. Due to there are 2 stalagmites composed, we choose 4 drilling position for dating (Fig.35).

Sample name	Shape	Color		Texture	
		External	Internal	External	Internal
BR 1	Nearly symmetrical candle shape	Greyish yellow	- Light color in the upper part - Dark layers dominate the lower part	- Weathered/rough surface - Visible macroholes	- Many small cavities - Shifted growth axis in the uppermost part
BR 2	Nearly symmetrical candle shape with larger diameter in the middle part	Greyish yellow	- Lighter colors than BR1 sample - Interfingered darker band with lighter band	- More irregular/rougher than BR 1 - Visible macroholes	- Growth axis shifted ostensibly in the uppermost part - Many cavities along the growth layers in the lower part.
BR 3	Composed of 2 stalagmites - Outer: symmetry- - Inner: symmetrical cone-like shape	Greyish yellow but lighter than BR 1 and BR 2	- Lighter colors than BR1-2 sample - Interfingered darker band with lighter band	- Outer: rough and corroded - Inner: rough and corroded	- Discontinuity layer between inner and outer stalagmite. - Both also show cavities along some growth layers - Different growth axis direction.

Table2. Summary of physical properties of 3 samples.

3.2 Chronology

After we select the drilling position and get the powder (c. ~20 mg) of sample from drilling process. Then, we do the chemistry lab to get rid of the unnecessary element and separate the uranium and thorium from each other. The ages were measured by MC-ICP-MS machine. The measured values of uranium-thorium concentration and aged calculation show as the table3. The calibrated ages of all samples are in a part of Pleistocene epoch (2.58 Ma – 11.7 Ka). BR 1 has the age from 89479-90871 and the error range from ± 971-7728 yr, BR 2 has the age from 88845-87574 and the error range from ± 1363-1552 yr. BR 3 (inner stalagmite) has the age from 96313-96710 and the error range from ± 2639-6809 yr. BR 3 (outer) has the age at the top point is 97308 ± 1590 yr, so the age in each point is an average age from replicated measurement. According to the age on top and bottom in each sample. The age is overlapped with each other. Thus, the results of our data is not reliable as much as we expected.

Table3. ^{230}Th dating results of BR 1-3 Stalagmites from BR cave, Western Thailand. Measured by MC-ICP-MS and the error is 2s error.

Sample Number	^{238}U (ppb)		^{232}Th (ppt)		^{230}Th / ^{232}Th (atomic x10^{-6})		d^{234}U* (measured)		^{230}Th / ^{238}U (activity)		^{230}Th Age (yr) (uncorrected)		^{230}Th Age (yr) (corrected)		d^{234}U$_{Initial}$** (corrected)		^{230}Th Age (yr BP)*** (corrected)	
1A	181	±0	21239	±428	106	±2	177.6	±2.1	0.7560	±0.0027	108039	±732	**105253**	**±2096**	239	±3	105188	±2096
1B	180	±0	10042	±202	200	±4	179.9	±2.1	0.6791	±0.0023	90822	±548	**89494**	**±1084**	232	±3	89429	±1084
2A	119	±0	39624	±797	36	±1	144.7	±2.1	0.7263	±0.0032	106550	±859	**98117**	**±6042**	191	±4	98052	±6042
2B	116	±0	29348	±590	47	±1	157.4	±2.0	0.7146	±0.0028	101698	±716	**95434**	**±4493**	206	±4	95369	±4493
3A	85	±0	32395	±650	31	±1	157.8	±2.0	0.7228	±0.0028	103519	±720	**93990**	**±6809**	206	±5	93925	±6809
3B	82	±0	12161	±244	78	±2	155.4	±2.0	0.7017	±0.0023	99080	±596	**95443**	**±2639**	203	±3	95378	±2639
4A	48	±0	10654	±214	53	±1	164.3	±1.9	0.7216	±0.0028	102217	±716	**96731**	**±3948**	216	±3	96666	±3948
4B	47	±0	9754	±196	56	±1	161.2	±2.1	0.7148	±0.0028	101154	±727	**96025**	**±3700**	211	±4	95960	±3700
5A	84	±0	26951	±541	35	±1	144.4	±2.1	0.6777	±0.0029	95379	±711	**87227**	**±5826**	185	±4	87162	±5826
5B	75	±0	9403	±189	87	±2	149.7	±2.1	0.6617	±0.0026	91173	±618	**88052**	**±2289**	192	±3	87987	±2289
6A	89	±0	7334	±148	131	±3	145.3	±2.1	0.6576	±0.0023	90918	±567	**88868**	**±1552**	187	±3	88803	±1552
6B	89	±0	6498	±130	149	±3	146.5	±1.6	0.6576	±0.0021	90749	±500	**88952**	**±1363**	188	±2	88887	±1363
7A	78	±0	30562	±615	30	±1	132.7	±2.1	0.7102	±0.0023	104684	±653	**94529**	**±7248**	173	±4	94464	±7248
7B	75	±0	31411	±631	27	±1	138.5	±2.1	0.6862	±0.0032	98153	±798	**87343**	**±7728**	177	±5	87278	±7728
8A	44	±0	2806	±57	172	±4	143.7	±2.0	0.6575	±0.0032	91115	±729	**89553**	**±1317**	185	±3	89488	±1317
8B	40	±0	1575	±32	273	±6	146.7	±1.9	0.6566	±0.0030	90512	±690	**89535**	**±971**	189	±3	89470	±971

U decay constants: l_{238} = 1.55125x10^{-10} (Jaffey et al., 1971) and l_{234} = 2.82206x10^{-6} (Cheng et al., 2013). Th decay constant: l_{230} = 9.1705x10^{-6} (Cheng et al., 2013).*d^{234}U = ([^{234}U/^{238}U]$_{activity}$ – 1)x1000. ** d^{234}U$_{initial}$ was calculated based on ^{230}Th age (T), i.e., d^{234}U$_{initial}$ = d^{234}U$_{measured}$ x e^{l234xT}. Corrected ^{230}Th ages assume the initial ^{230}Th/^{232}Th atomic ratio of 4.4 ±2.2 x10^{-6}. Those are the values for a material at secular equilibrium, with the bulk earth ^{232}Th/^{238}U value of 3.8. The errors are arbitrarily assumed to be 50%. ***B.P. stands for “Before Present” where the “Present” is defined as the year 1950 A.D.

Chapter 4

Discussions

4.1 Physical properties assessment

We used to assume that the crystal in stalagmite is compacted but actually the cavity has always exist as post-depositional and digenesis features in some case (e.g. Frisia, 1996). Normally in precipitation process of calcite, drips water should be supersaturated that lead the equilibrium more than 1 like the equation below. But if the equilibrium is less than 0, post-deposional features will form—dissolution or diagenetic/secondary porosity (Shtober-Zisu et al., 2014).

$$\Omega_{ct} = \log [K_{sp}/a_{cos}{}^{*}a_{ca}] \quad > \quad 0$$

These process can cause by undersaturated or acidic dripping water with high value of pCO_2 of external influenced (Perrin et al., 2014), abruptly increasing drips water rate which prevented sufficient degassing to bring feeding water to equilibrium with $CaCO_3$ (Railsb ack et al. 2011; Railsback et al. 2013). Agreeable with Scholz et al (2014) which presented 4 scenarios of dissolution water. (1) Mixing dissolution solution that means the drips water source are more than one. (2) pCO_2 of cave higher than epikarst that cause by changed the density of soil or glacial/stadial conditions. (3) Fast flow rate which can change the supersaturated to undersaturated drip water. (4) Changing open to closed-system.

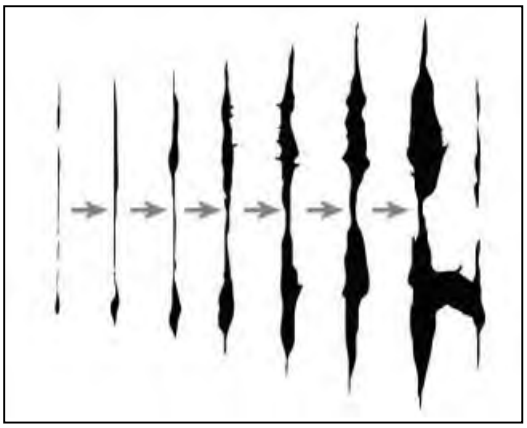

Figure 36. Sketch illustrating the gradual opening of secondary voids in the primary columnar calcite.

According to elongate dissolution, this process affects to primary columnar calcite and is initiated particularly as elongated cavities long the boundaries between neighboring crystals. Such secondary voids are enlarged gradually by the ongoing dissolution process,

and their width varies from a few micrometers to a few hundreds of micrometers. Finally in advanced stage, these dissolution cavities are connected to each other and form a frame of microholes in the central part of the stalagmite (Perrin et al., 2014). Regarding to Figure.37 and 38, even its central voids is not long that much but it shows a little bit depression downward and across the layers. So that may cause by undersaturated or corrosive water cut through the growth layers along microfractures inside as Off axis holes (OAHs) which shows both internal and external structure (Shtober-Zisu et al., 2014). Moreover, linear or elongate dissolution is the characteristic of bacterial activity (Railsback et al., 1994). Likewise, some microorganisms can enhance the dissolution following the equation below. The final product is HCO_3^- , weak acid, that can cause the dissoltion.

Figure 37. Cavities in BR 1 (lower part; right).

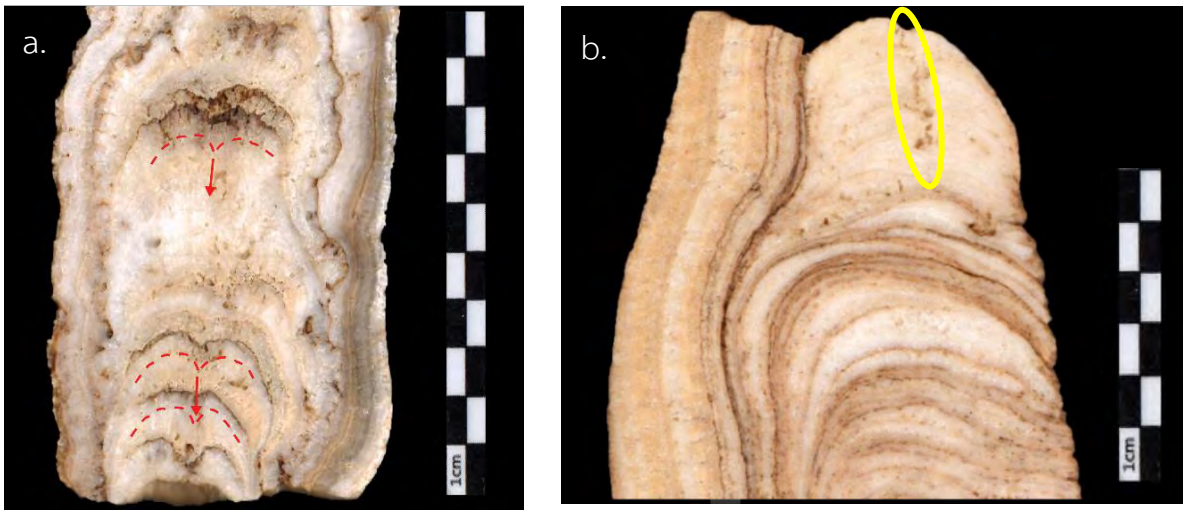

Figure 38. (a.) Cavities in BR 2 (lower part; left) (b.) Cavities in BR 2 (lower part; right).

As you can see in chapter 3 (Fig. 30a, 33a, and 34a), the observation shows the surface and inner skin of all samples. Rough and weathered skin can see distinctively. This may also cause by dissolution process.

$$CH_2O(org) + O \longrightarrow H_2O + CO_2$$
$$CO_2 + H_2O \longrightarrow H^+ + HCO_3^-$$
$$H^+ + CaCO_3 \longrightarrow Ca^{2+} + HCO_3^-$$

In the term of corrosion that means oxidation of a metal and cannot be applied to the dissolution of calcium carbonate. The processes occur when air equilibrating with cave atmosphere produces condensed moisture over the cave walls and speleothems (Perrin et al., 2014). As you can see in Figure 39, the brownish red short layers may cause by oxidation process. Table 4 shows the metal elements which studied by Electron Probe micro-analyzer (EPMA) at department of geology, faculty of science, Chulalongkorn university. We assume that caused by oxidation of iron oxides siderite ($FeCO_3$) as the equation are showed below.

Siderite to Magnetite in closed system

$$FeFe_2O_4 + 3HCO_3^- + 5H^+ + 2e^- \longrightarrow 3FeCO_3 + 4H_2O$$

Siderite to Hematite in closed system

$$Fe^{3+}{}_2O_3 + 2HCO_3^- + 4H^+ + 2e^- \longrightarrow 2FeCO_3 + 3H_2O$$

Oxidation of siderite to magnetite

$$Fe^{2+}Fe^{3+}{}_2O_4 + 2e^- \longrightarrow 3Fe^{2+} + CO_3$$

In a wet environment

$$Fe_3O_4 + 3CO_2 + 2H^+ + 2e^- \longrightarrow 3FeCO_3 + H_2O$$

	F	Mg	Ca	Pb	Fe	Al	Na	Sr	Zn	Mn	Si	Total	Comment
ppm	0	436.6667	397426.7	200	15170	0	70	0	546.6667	0	2736.667	416620	2-1-cal-1

Table 4. Shows quantity of average element of point 10-11-12 of Warisa's study (Fig.39).

Figure 39. Illustrates the oxidation layer on BR 2; the upper right part (3.1 cm from top)

Figure 40. Shows the discontinuity layer as red, yellow, green, and blue lines on BR 2; upper right part.

In addition, the growth discontinuity in Figure 40 (red, yellow, green, and blue lines) draws by the different of growth axis that causes by changing of drip water fissures that feeding the stalagmite—decrease or stop of drip water or lower intensity of degassing(Perrin et al., 2014). Thus, these discontinuity may imply the hiatus event that change the quality of drip water and becoming undersaturated water which cause of dissolution process simultaneously.

On the other hand, these discontinuity layers have to be dated and correlate with other layer to understand the age evolution.

As a consequence, BR 3 is the most favorable of all samples because there are consist of two stalagmites that is very interesting because the discontinuity layer between two stalagmites looks much altered. These make they separated easily after cutting. So there will be an ambiguous event from external environment that influenced to this cave. Even though BR 1 and 2 are nearly symmetry shape but they compose of many dissoluted cavities that make the BR 3 looks better. However, the age of BR3 shows quite big errors that means the physical properties cannot ensure the potential of sample directly.

4.2 Uncertainly errors and uranium-thorium content

According to the drilling point, top and bottom of the samples were selected for dating because we are interesting in time interval of the sample. Drilling points should be close to growth axis and constrain potential hiatuses and coarely crystalline is prefered (H. Cheng et al., 2013). According to Table 5, our error ranges from ±971 to ±7728 a. but normally the MC-ICP-MS at Earth Observatory of Singapore (EOS) is very high resolution and errors should be in ±1-2‰ (2σ) for abundance determination of ~20 fg ^{234}U or ^{230}Th that mean the error should be ±100 a. at 130 ka (H. Cheng et al., 2013). The large error lead the top and bottom age overlap with each other that make the results are difficult to work further.

Sample Number	^{230}Th Age (yr BP) *** (corrected)		Percent errors
1A	105188	±2096	1.99 %
1B	89429	±1084	1.21 %
2A	98052	±6042	6.16 %
2B	95369	±4493	4.71 %
3A	93925	±6809	7.24 %
3B	95378	±2639	2.76 %
4A	96666	±3948	4.08 %
4B	95960	±3700	3.85 %
5A	87162	±5826	6.68 %
5B	87987	±2289	2.60 %
6A	88803	±1552	1.74 %
6B	88887	±1363	1.53 %
7A	94464	±7248	7.67 %
7B	87278	±7728	8.85 %
8A	89488	±1317	1.47 %
8B	89470	±971	1.08 %

Table 5. Shows percent errors of ^{230}Th Age

	^{230}Th / ^{232}Th (atomic ratio; ppm)	^{238}U (ppb)
This study	**27 – 273**	**40 - 181**
Fleitmann et al., 2007	2 – 3080	300 - 9000
L. Tan et al., 2009	59 – 4527	12400 - 21800
Cai et al., 2010	17	1180
Muangsong et al., 2011	6.7 - 17	1000 - 1450
L. Tan et al., 2013	3.5 - 84.9	3600 - 4900
Muangsong et al., 2014	108 – 611	2800 - 3300

Table 6. Comparison of ^{230}Th / ^{232}Th ratio and ^{238}U content of our study with others.

The large error is discussed by unsuitable of uranium and thorium concentration. According to uranium and thorium concentration, our ^{230}Th / ^{232}Th ratio ranges 27-273 ppm and ^{238}U ranges 40-181 ppb. In the good view, ^{230}Th / ^{232}Th ratios should not be low because it probably contain of detrital materials that lead ambiguously to larger of error and ^{238}U should be rich at least 100-200 ppb (H. Cheng et al., 2013). As ^{238}U decay series, only ^{238}U is soluble and came with drip water, then decayed following its series to ^{232}Th that means decreasing of ^{238}U concentration when it get older and increasing of ^{230}Th concentration. According to Table 5, our ^{230}Th / ^{232}Th ratio is not far from others study that much but our ^{238}U concentration is very low. Our ^{230}Th is too low and ^{232}Th is too high that make the ratio get lower than expected.

Thorium is rapidly absorbed onto particles (Ivanovich and Harmon, 1992; Milne et al., 2003) therefore we often found thorium surrounding $CaCO_3$ matrix during the dissolution process of calcite. Scholz et al (2014) stated that uranium and thorium are neither lost nor added after deposition and whatever it will disturb the “U-Th clock” and alter ^{230}Th/U-ages. Especially ^{232}Th which common in natural and very high in our samples (see Table 3), means that our sample was invasive by open system. Regarding to uranium,

the reprecipitation may have a different ^{234}U / ^{238}U activity ratio than $CaCO_3$ initial matrix that also lead to error of $^{230}Th/U$-ages. Moreover, timing, duration, and amount of uranium loss and addition are also the considered parameters.

4.3 Oil supported cutting

Figure 41. Shows the altered sample of BR 3 (lower part; left) and BR 2 (lower part; left) after cutting

Our cutting process was done at department of geology, faculty of science, Chulalongkorn University. The unclean process and tools might be causes of errors results. The dirty oil might be interact with the sample through the porosity. Unpleasant smell occurred after cutting process until washing process at Earth Observatory of Singapore (EOS). By now after we test the sample and keep it for a while (2-3 months), the samples still smell bad and get more dirty than ever (Fig.41). So we assume that it's very interesting to study further.

Chapter 5

Conclusion

Following from the previous chapter, our samples are composed of dissolution features, corrosion features, and several discontinuity layers. These may represent the large error of age and improper of uranium and thorium concentration. Due to the ages are not reliable, our samples are not suitable for paleoclimatic study.

This study is just preliminary process for paleoclimate implication because the process cannot step further after the dating result was failed. The assessment of physical properties such as dissolution features will guide the researcher for collecting a sample in the future. Even the physical properties cannot ensure the proper sample efficiency. But if our samples look clean or not follow the unwanted characteristics as we discussed previously, we will get more confident with the dating in the next.

As you know, the first published stalagmites sample for climate implication in Thailand belongs to Cai et al., 2010. The ages of their stalagmites cover 306-2005 A.D that are very young but our samples are very old. That means the stalagmites in Thailand have a wide range and very useful for paleoclimate study. In addition, all of our samples has the ages in near range so that means Banrai cave was activated just temporary and inactivated for long times until the present or there are some stalagmites in this cave but undiscovered. In our survey field in nearly Banrai cave also found both of active and inactive cave. The inactive cave can see easily that the humidity is very low, the entrance is wide, and the route is short and well known to people. The active cave is opposites of inactive cave ostensibly. There is a small or narrow entrance, the route is long and composes of many chambers, and humidity is very high which you can feel the cold air and less of air circulation. Likewise, our survey field is just a little area of carbonate mountains in the western region and has a plenty of area are unexplored.

In addition, oil supported cutting is not recommended because its result after cutting is quiet dirty. However, we have not studied further with the dirty samples yet. It should be studied in micro-scale and discussed of its causes.

Eventually, this is oldest stalagmite study in Thailand until now. We believe that this area still has a potential to study and several speleothems are waiting for us. Thailand is complicated climate area and we still scarce of data. We hope this study will attract people to realize in our resources, our problem, and how we can utilize our treasures efficiency.

REFERENCES

Cai, B., Pumijumnong, N., Tan, M., Muangsong, C., Kong, X., Jiang, X., & Nan, S., 2010. Effects of intraseasonal variation of summer monsoon rainfall on stable isotope and growth rate of a stalagmite from northwestern Thailand. J. Geophys. Res. Journal of Geophysical Research, 115(D21).

Cheng, H., Edwards, R., Hoff, J., Gallup, C., Richards, D., & Asmerom, Y., 2000. The half-lives of uranium-234 and thorium-230. Chemical Geology, 169(1-2), 17-33.

Cheng, H., Edwards, R. L., Shen, C., Polyak, V. J., Asmerom, Y., Woodhead, J., Hellstrom, J., Wang, Y., Kong, X., Spötl, C., Wang, X., & Alexander, E. C., 2013. Improvements in 230Th dating, 230Th and 234U half-life values, and U–Th isotopic measurements by multi-collector inductively coupled plasma mass spectrometry. Earth and Planetary Science Letters, 371-372, 82-91.

Dorale, J. A., Edwards, R. L., Jr, E. C., Shen, C., Richards, D. A., & Cheng, H., 2004. Uranium-Series Dating Of Speleothemes: Current Techniques, Limits amp; Applications. Studies of Cave Sediments, 177-197.

Dykoski, C., Edwards, R., Cheng, H., Yuan, D., Cai, Y., Zhang, M., Lin, Y., Qing, J., An, Z., & Revenaugh, J., 2005. A high-resolution, absolute-dated Holocene and deglacial Asian monsoon record from Dongge Cave, China. Earth and Planetary Science Letters, 233(1-2), 71-86.

Fairchild, I. J., Smith, C. L., Baker, A., Fuller, L., Spötl, C., Mattey, D., McDermott, F., E.I.M.F., 2006. Modification and preservation of environmental signals in speleothems. Earth- Science Reviews, 75(1-4), 105-153.

Fairchild, I. J., Frisia, S., Borsato, A., & Tooth, A. F., 2006. Speleothems. Geochemical Sediments and Landscapes, 200-245.

Fairchild, I. J., & Treble, P. C., 2009. Trace elements in speleothems as recorders of environmental change. Quaternary Science Reviews, 28(5-6), 449-468.

Fleitmann, D., Burns, S. J., Neff, U., Mudelsee, M., Mangini, A., & Matter, A., 2004. Palaeoclimatic interpretation of high-resolution oxygen isotope profiles derived from annually laminated speleothems from Southern Oman. Quaternary Science Reviews, 23(7-8), 935-945.

Fleitmann, D., Burns, S. J., Mangini, A., Mudelsee, M., Kramers, J., Villa, I., Neff, U., Al-Sbubbary, A. A., Busttner, A., Hippler, D., & Matter, A., 2007. Holocene ITCZ and Indian monsoon dynamics recorded in stalagmites from Oman and Yemen (Socotra). Quaternary Science Reviews, 26(1-2), 170- 188.

Fleitmann, D., Spötl, C., Newman, L., & Kiefer, T., 2008. Advances in Speleothem Research. PAGES News, 16, 1-40.

Frank, N., Braum, M., Hambach, U., Mangini, A., & Wagner, G., 2000. Warm Period Growth of Travertine during the Last Interglaciation in Southern Germany. Quaternary Research, 54(1), 38-48. doi:10.1006/qres.2000.2135

Geyh, M., 2008. Selection of Suitable Data Sets Improves 230Th/U Dates of Dirty Material. Geochronometria, 30(-1).

Hellstrom, J., 2006. U–Th dating of speleothems with high initial 230Th using stratigraphical constraint. Quaternary Geochronology, 1(4), 289-295.

Lauritzen, S., & Lundberg, J., 1999. Speleothems and climate: A special issue of The Holocene. The Holocene Holocene, 9(6), 643-647.

Mcdermott, F., Frisia, S., Huang, Y., Longinelli, A., Spiro, B., Heaton, T. H., Hawkesworth, J. C., Borsato, A., Keppens, E., Fairchild, J. I., Borg, v. K., Verheyden, S., & Selmo, E., 1999. Holocene climate variability in Europe: Evidence from δ18O, textural and extension-rate variations in three speleothems. Quaternary Science Reviews, 18(8-9), 1021-1038.

Mcdermott, F., 2004. Palaeo-climate reconstruction from stable isotope variations in speleothems: A review. Quaternary Science Reviews, 23(7-8), 901-918.

Muangsong, C., Pumijumnong, N., Cai, B., & Tan, M., 2011. Stalagmite grey level as a proxy of the palaeoclimate in northwestern Thailand. ScienceAsia, 37, 262-267.

Muangsong, C., Cai, B., Pumijumnong, N., Hu, C., & Cheng, H., 2014. An annually laminated stalagmite record of the changes in Thailand monsoon rainfall over the past 387 years and its relationship to IOD and ENSO. Quaternary International, 349, 90-97.

Muñoz-García, M., López-Arce, P., Fernández-Valle, M., Martín-Chivelet, J., & Fort, R., 2012. Porosity and hydric behavior of typical calcite microfabrics in stalagmites. Sedimentary Geology, 265-266, 72-86.

Perrin, C., Prestimonaco, L., Servelle, G., Tilhac, R., Maury, M., & Cabrol, P., 2014. Aragonite-Calcite Speleothems: Identifying Original and Diagenetic Features. Journal of Sedimentary Research, 84(4), 245-269.

Railsback, L. B., Akers, P., Wang, L., Holdridge, G., & Voarintsoa, N. R., 2013. Layer-bounding surfaces in stalagmites as keys to better paleoclimatological histories and chronologies. International Journal of Speleology IJS, 42(3), 167-180.

Scholz, D., Tolzmann, J., Hoffmann, D. L., Jochum, K. P., Spötl, C., & Riechelmann, D. F., 2014. Diagenesis of speleothems and its effect on the accuracy of 230Th/U-ages. Chemical Geology, 387, 74-86.

Shen, C., Edwards, R. L., Cheng, H., Dorale, J. A., Thomas, R. B., Moran, S. B., Weinstein, E. S., & Edmonds, H. N. (2002). Uranium and thorium isotopic and concentration measurements by magnetic sector inductively coupled plasma mass spectrometry. Chemical Geology, 185(3-4), 165-178.

Shen, C., Lin, H., Chu, M., Yu, E., Wang, X., & Dorale, J. A., 2006. Measurements of natural uranium concentration and isotopic composition with permil-level precision by inductively coupled plasma-quadrupole mass spectrometry. Geochemistry, Geophysics, Geosystems Geochem. Geophys. Geosyst., 7(9).

Shen, C., Li, K., Sieh, K., Natawidjaja, D., Cheng, H., Wang, X., Edwards, L. R., Lam, D. D., Hsieh, T. Y., Fan, Y. T., Meltzner, J. A., Taylor, W. F., Quinn, M. T., Chiang, H., & Kilbourne, K. H., 2008. Variation of initial 230Th/232Th and limits of high precision U–Th dating of shallow-water corals. Geochimica Et Cosmochimica Acta, 72(17), 4201-4223.

Shen, C., Wu, C., Cheng, H., Edwards, R. L., Hsieh, Y., Gallet, S., Chang, C., Li, T., Lam, D. D., Kano, A., Hori, M., & Spötl, C., 2012. High-precision and high-resolution carbonate 230Th dating by MC-ICP-MS with SEM protocols. Geochimica Et Cosmochimica Acta, 99, 71-86.

Shen, C., Lin, K., Duan, W., Jiang, X., Partin, J. W., Edwards, R. L., Cheng, H., & Tan, M., 2013. Testing the annual nature of speleothem banding. Sci. Rep. Scientific Reports, 3.

Shtober-Zisu, N., Schwarcz, H., Chow, T., Omelon, C., & Southam, G., 2014. Caves in caves: Evolution of post-depositional macroholes in stalagmites. International Journal of Speleology IJS, 43(3), 323-334.

Singhrattna, N., Rajagopalan, B., Kumar, K. K., & Clark, M., 2005. Interannual and Interdecadal Variability of Thailand Summer Monsoon Season. Journal of Climate J. Climate, 18(11), 1697-1708.

Southon, J., Noronha, A. L., Cheng, H., Edwards, R. L., & Wang, Y., 2012. A high-resolution record of atmospheric 14C based on Hulu Cave speleothem H82. Quaternary Science Reviews, 33, 32-41.

Spötl, C., & Boch, R., 2012. Uranium Series Dating of Speleothems. Encyclopedia of Caves, 838-844.

Tan, L., Orland, I. J., & Cheng, H., 2014. Annually laminated speleothems in paleoclimate studies. PAGES MAGAZINE, 22, 22-23.

Tan, L., Cai, Y., Cheng, H., Edwards, R. L., Shen, C., Gao, Y., & An, Z., 2015. Climate significance of speleothem δ18O from central China on decadal timescale. Journal of Asian Earth Sciences, 106, 150-155.

Tremaine, D. M., & Froelich, P. N., 2013. Speleothem trace element signatures: A hydrologic geochemical study of modern cave dripwaters and farmed calcite. Geochimica Et Cosmochimica Acta, 121, 522-545.

Wang, Y. J., Cheng, H., Edwards, R. L., An, Z. S., Wu, J. Y., Shen, C. -., & Dorale, J. A., 2001. A High-Resolution Absolute-Dated Late Pleistocene Monsoon Record from Hulu Cave, China. Science, 294(5550), 2345-2348.

Yuan, D., 2004. Timing, Duration, and Transitions of the Last Interglacial Asian Monsoon. Science, 304(5670), 575-578.

Zhang, H., Yu, K., Zhao, J., Feng, Y., Lin, Y., Zhou, W., & Liu, G. (2013). East Asian Summer Monsoon variations in the past 12.5ka: High-resolution δ18O record from a precisely dated aragonite stalagmite in central China. Journal of Asian Earth Sciences, 73, 162-175.